Modulation of tooth regeneration through opposing responses to Wnt and BMP signals in teleosts

Tyler A. Square[1], Emma J. Mackey[1,2], Zoe Z. Chen[1], Shivani Sundaram[1,3], Craig T. Miller[1]

[1] Department of Molecular & Cell Biology, University of California, Berkeley, California USA
[2] Present address: Department of Biochemistry, University of Washington, Seattle, Washington USA
[3] Present address: Keck School of Medicine, University of Southern California, Los Angeles, California USA

Abstract

Most vertebrates are capable of regenerating entire tooth organs. Tooth regeneration has long been hypothesized to rely on extracellular signals that can influence multiple tooth sites at once. Little is known about which secreted signaling molecules can influence this process. As an entry point, we asked whether fish orthologs of genes known to regulate mammalian hair regeneration have effects on tooth regeneration or total tooth number. We tested whether tooth regeneration could be accelerated by exogenous Wnt signaling (via *Wnt10a*) or BMP inhibition (*Grem2a*), and if regeneration rates were slowed by exogenous BMP signaling (*Bmp6*) or Wnt inhibition (*Dkk2*). Using two fish species that demonstrate distinct modes of whole tooth regeneration, the threespine stickleback (*Gasterosteus aculeatus*) and zebrafish (*Danio rerio*), we found that transgenic overexpression of four different genes changed tooth replacement rates in the predicted direction: *Wnt10a* and *Grem2a* increased the tooth replacement rate, while *Bmp6* and *Dkk2* strongly inhibited replacement tooth formation. Regulation of total tooth number was separable from regulation of regeneration rates. In zebrafish, none of the factors affecting regeneration rate affected the number of distinct tooth families but did sometimes affect total tooth number. In sticklebacks, which do not exhibit clear tooth families, *Bmp6* and *Dkk2* reduced total tooth number, while *Wnt10a* and *Grem2a* did not. These data support a model where different epithelial organs like teeth and hair share genetic inputs driving the timing of whole organ regenerative cycles.

Introduction

Tooth regeneration is a trait demonstrated by most vertebrate groups[1–3]. This regenerative process usually takes the form of whole tooth replacement, where entire new tooth organs differentiate while old teeth are removed by active shedding and/or dislodgement through use. Tooth replacement events often exhibit a high degree of within-species consistency with respect to their timing, sequence, and spacing, forming characteristic replacement patterns. This consistency has led to hypotheses that neighboring or alternating tooth positions could be subject to signals that act to influence or coordinate the timing of regeneration cycles for multiple teeth in tandem[4–9]. The potential involvement of secreted signals in tooth regeneration is additionally suggested by studies on primary tooth differentiation, where the functional relevance of numerous signaling ligands has been documented[10–22]. However, little is known about which secreted signals can regulate the process of whole tooth regeneration.

Whole organ regeneration is a trait that teeth share with many other epithelial appendages. This class of organs includes body coverings like hair, scales, and feathers, and some soft organs like salivary glands and sweat glands[23–25]. Whether regeneration is cyclic and programmed or only brought on by injury or wear, nearly all types of epithelial appendages can be wholly replaced via regeneration[26–33]. Despite the stark differences in their basic compositions as mature organs, different epithelial appendages demonstrate numerous developmental genetic similarities, in some cases suggesting deep homology or even direct homology between these organs[24,34–41]. Given that most epithelial organs demonstrate the capacity to regenerate, we parsimoniously hypothesize that these regenerative processes are driven by shared genetic networks. We previously tested this idea by looking at fine-scale gene expression during zebrafish and stickleback tooth regeneration[42]. This study found that ten hair follicle stem cell marker candidate genes demonstrated orthologous gene expression in both zebrafish and stickleback successional dental epithelia (SDE), including *CD34, Gli1, Nfatc1*, and

Bmp6. This battery of gene expression marks the epithelia presaging tooth and hair regeneration in their respective cellular contexts, suggesting a remarkable level of genetic overlap in these naïve tissues.

In the present work, we aimed to test whether genetic mechanisms known to drive hair regeneration could similarly influence tooth regeneration in sticklebacks and zebrafish. In mammalian hair, some secreted factors have been identified as likely or possible regulators of hair follicle stem cells. Namely, a Wnt-BMP cycling mechanism has been well supported, whereby the Wnt and BMP pathways have oppositional roles that drive the oscillation of the hair regenerative cycle between active growth (anagen, high Wnt + BMP inhibitors) and quiescence (telogen, high BMP + Wnt inhibitors)[26,43–45]. Ligands implicated in promoting hair regeneration include Wnt ligands, Wnt10a, Wnt10b, Wnt7a, and Wnt7b, as well as specific BMP inhibitors Grem1, Grem2, Bambi, and Noggin1[11,43,44,46–49]. Conversely, secreted BMP signals like Bmp2, Bmp4, Bmp6, and Wnt inhibitors like Dkk1 and Dkk2 have been implicated in slowing or stopping the regenerative process[26,43,44,50–52]. To test whether such secreted ligands could elicit congruent changes in the regeneration rates of teeth, we selected four of the above genes (*Wnt10a*, *Dkk2*, *Bmp6*, and *Grem2a*) to test for both endogenous expression in actively regenerating tooth fields, and their possible effects on both tooth replacement rates and total tooth number. Our selection of specific gene orthologs was partly motivated by known pleiotropic disease loci in humans: *WNT10A* and *GREM2* are known to be associated with different forms of ectodermal dysplasia, where both tooth and hair regeneration are perturbed, but not always primary epithelial organ growth[11,53]. *Grem2* loss-of-function has been shown to disrupt constant incisor outgrowth in mice[14]. *Bmp6* has been strongly implicated in both mouse hair regeneration[43,44] and the natural evolution of stickleback tooth regeneration rates and total tooth number[54,55]. *Dkk2* expression has been shown to oscillate during the regenerative cycle in the hair follicle[52] and is sufficient to cause ectopic hair to grow in normally hairless regions of

mouse skin[56]. All four of these selected genes demonstrate substantial expression levels in a previously published RNAseq dataset derived from late-stage stickleback tooth fields undergoing regeneration[57], suggesting these genes could regulate tooth regeneration. Furthermore, stimulation of downstream Wnt signaling via a constitutively active β-catenin (*Ctnnb*) has been shown to induce replacement events in mouse molars, a process which normally does not occur in this species, suggesting that Wnt upregulation indeed plays a crucial role in promoting whole tooth organ regeneration[58,59].

Results

Expression of secreted ligand genes of interest in stickleback

We examined *Wnt10a*, *Dkk2*, *Bmp6*, and *Grem2a* expression in wild-type subadult stickleback pharyngeal tooth fields (Fig. 1). We documented expression not just in tooth organs themselves, but also the regions between teeth, as these could also be involved with regulating tooth organ development or regeneration. Overall, we found that all four genes are expressed both in developing tooth organs and in epithelial and/or mesenchymal cell populations surrounding tooth organs.

Wnt10a transcripts were detected in early bud-stage tooth germs in both the epithelium and the earliest tooth mesenchyme, as previously published (Fig. 1A). Epithelial expression was also observed at the late-bell stage, favoring the inner dental epithelium (Fig. 1B-D). *Wnt10a* Expression in dental mesenchyme persists through eruption (Fig. 1C) but is not appreciably detected in fully ankylosed and erupted teeth (Fig. 1D). *Wnt10a* is also detected in isolated regions of epithelial and mesenchymal cells at other locations in the tooth field, most often in mesenchyme near or below developing tooth germs (Fig. 1A-C, brackets).

The Wnt signaling inhibitor *Dkk2* was diffusely expressed in the epithelium overlying the entire tooth field (Fig. 1E and F). Increased epithelial expression detected in bell-stage tooth organs, especially in the inner dental epithelium (Fig. 1E). In tooth mesenchyme, we first detected expression in the early bell stage (Fig. 1E), which appears to persist through tooth differentiation, including in odontoblasts located towards the apex (tip) of the tooth in fully ankylosed and erupted teeth (Fig. 1F). *Dkk2* was additionally observed in deep mesenchymal cell populations between teeth, against the bone of attachment that serves as the anchor for ankylosed teeth (Fig. 1E, bracket).

Bmp6 was expressed similarly to *Wnt10a* in bud-stage teeth, exhibiting focal expression in both the epithelium and mesenchyme (Fig. 1G). As previously published, Bmp6 was detected in the inner dental epithelium and mesenchyme of bell-stage tooth germs (Fig. 1H), and mesenchymal expression is maintained during and after eruption (Fig. 1I and J). *Bmp6* expression was detected at a subset of successional dental epithelium (SDE) locations as well as isolated clusters of mesenchymal cells surrounding teeth in the tooth field (Fig. 1I).

The BMP inhibitor *Grem2a* was detected in mesenchyme adjacent to bud stage tooth germs but appeared to be excluded from the epithelium and dense mesenchymal condensation of the early tooth germ itself (Fig. 1K). During bell stages, tooth germs exhibited both inner and outer dental epithelial expression as well as mesenchymal expression (Fig. 1L and M), all of which was also present in eruption stage teeth (Fig. 1M). Fully ankylosed and erupted teeth maintained mesenchymal expression in odontoblasts (Fig. 1M). *Grem2a* transcripts were additionally detected in the SDE, in other dispersed epithelial cells (Fig. 1M), and in mesenchymal cells surrounding teeth and tooth organs in the tooth field (Fig. 1K-M).

Pulse-chase bone labeling and gene overexpression approach

Three of the four secreted ligand genes we focus on here are required for normal primary tooth development in different species (*Wnt10a*[10,11], *Bmp6*[55], and *Grem2a*[14,53]). Such early requirements present obstacles to using germline loss-of-function mutations to understand gene functions in late-stage tooth fields, because alterations to early primary tooth differentiation likely confound interpretations of later events like regeneration. We thus sought a genetic system that could test the effects of secreted Wnt and BMP pathway members of interest during late developmental stages without interfering with tooth field initiation and early primary tooth differentiation. Heat shock gene overexpression (OE) is as attractive option because it is temporally inducible during late developmental timepoints and well established in zebrafish[60,61]. The strategy we used thus couples OE treatments of *Wnt10a*, *Dkk2*, *Bmp6*, or *Grem2a* with a two-color pulse-chase bone staining protocol (summarized in Fig. 2), allowing us to classify each tooth in each individual as either “new” or “retained” with respect to the OE treatment interval (see Methods). By calculating the new:retained tooth ratio for each fish, we invoke a simple proxy of each individual’s “tooth replacement rate,” which addresses whether changes to the pace of the regenerative cycle have occurred. For both species, we sum all new and retained teeth to assess “total tooth number,” a count that includes both erupted functional teeth and unerupted bony tooth germs. In sticklebacks this encompasses both oral and pharyngeal teeth usually numbering ~200-300, whereas zebrafish have just one pair of pharyngeal tooth fields with ~25-30 total teeth. Since zebrafish exhibit morphologically stationary tooth families with a stereotypical number and arrangement that is reached during early juvenile stages (~30 days old)[62], we additionally ask whether OE treatments can modify the number of tooth families present in zebrafish.

Wnt pathway modulation by overexpression of *Wnt10a* and *Dkk2*

We first sought to test whether positive regulation of the Wnt pathway could influence tooth regeneration or total tooth number. Due to the known requirement of WNT10A in human EA development and regeneration, and expression in early tooth fields across many vertebrates, we asked whether *Wnt10a* is sufficient to promote tooth replacement rate or total tooth number in stickleback and zebrafish (Fig. 3A). *Wnt10a* OE in sticklebacks simultaneously increased the number of new teeth (P=0.00072) and reduced the number of retained teeth (P=0.01), consistent with a role in promoting tooth regeneration. Together, these two shifts consistently raised the average new:retained tooth ratio (P=0.0003), as predicted. However, *Wnt10a* OE did not significantly change the total number of teeth (P=0.81), demonstrating that changes to the regeneration rate don't necessarily alter changes to total tooth number. These shifts are also generally reflected by most tooth field types alone (Fig. S1), suggesting generally consistent effects of this Wnt signaling ligand in both oral and pharyngeal tooth fields. Qualitatively, we noticed that the *Wnt10a* OE individuals oftentimes displayed uninterrupted clusters of five or more new teeth (Fig. 3C, dotted oval), whereas new tooth distribution in wild-type (WT) controls appeared more uniform.

We sought to determine whether the *Wnt10a* OE transgene could affect tooth replacement rates or total tooth number in carrier animals raised at normal temperatures. To test for these effects, we performed a negative control pulse-chase assay with the same staining interval (18 days) but with no intervening heat shocks, raising similar numbers of WT and transgene-carrying fish in the same tanks/conditions as the heat shock treatment but kept at normal temperatures (~17° C). Notably, these fish were full siblings to the treatment animals described above, helping to control for genetic variation. We found no significant deviation in the number of new teeth, number of retained teeth, the new:retained tooth ratio, and the total tooth number (Fig. S2).

We next tested *wnt10a* OE in zebrafish (Fig. 3D). Using the same 18 day pulse-chase overexpression assay, but with zebrafish resting and heat shock temperatures (see Methods and Fig. 2B), we found an increase in the number of new teeth formed during the treatment interval (*P*=0.00039). However, unlike sticklebacks, the number of retained teeth was unchanged (*P*=0.56). Overall the new:retained tooth ratio was significantly increased (*P*=0.0042). While we did not observe any change in the number of tooth families in any OE individual (n=15/15), we did find an increase in the total tooth number under *wnt10a* OE (*P*=0.011), due to a higher number of tooth families undergoing early replacement.

To address whether Wnt signaling inhibition could negatively influence tooth growth, we asked if Dkk2, a secreted Wnt signaling inhibitor, could decrease tooth replacement rates or total tooth number in sticklebacks (Fig. 4A). We found that Dkk2 OE strongly reduced the presence of new teeth (*P*=0.00024), while simultaneously increasing the presence of retained teeth (*P*=0.045). Together, these two effects led to a sharp decrease in the new:retained ratio (*P*=1.1e-5), while also decreasing the number of total teeth (*P*=0.0036). In the control condition, new teeth comprised mostly mid- or late bell stage tooth germs (Fig. 4B, arrows), whereas the few unankylosed new teeth we observed under Dkk2 OE were always at or near the eruption stage (Fig. 4C, arrow). These results are also generally reflected by each tooth field type alone (Fig. S3), although the oral tooth fields show a generally weaker response. To assess whether Dkk2 OE could be stalling tooth germs at stages prior to bone deposition (at bud, cap, or early-bell stages), we analyzed tooth field histology using H&E-stained sections (Fig. 4D and E). We found no evidence of bud, cap, or early-bell stage tooth germs across any pharyngeal tooth field we observed from Dkk2 OE individuals (n=7/7), suggesting that Dkk2 does not cause existing tooth germs to arrest during early differentiation.

BMP pathway modulation by overexpression of Bmp6 and Grem2a

We next sought to test whether modulation of Bmp signaling could affect tooth regeneration rates or total tooth number. Specifically, our hypothesis of a hair-like cycling mechanism operating in teeth predicts that tooth replacement should be inhibited by increases in BMP signaling and promoted by BMP inhibition. To test this hypothesis, we conducted a Bmp6 OE treatment, given known roles for Bmp6 in EA development and regeneration, including in stickleback teeth and mouse hair. Bmp6 OE produced a striking tooth phenotype unique among the phenotypes observed in this study: late bell (bony) tooth germs that were negative for both Alizarin Red and calcein (Fig. 5). We interpret these unstained tooth germs as “stalled,” i.e. tooth germs that initiated bone growth just after the Alizarin pulse/treatment onset, but ceased differentiation and bone deposition during the treatment interval and were thus no longer producing bone by the end of the treatment and the calcein chase. We conservatively counted these unstained, stalled tooth germs as assumed “new” teeth for this treatment, which were unique to Bmp6 OE and never otherwise observed. Even so, Bmp6 OE resulted in sharply reduced new tooth formation (*P*=2.7e-5, Fig. 6A). Surprisingly, Bmp6 OE also resulted in a decrease in retained teeth (*P*=2.8e-5), suggesting that Bmp6 negatively affects new tooth formation while also promoting the shedding of existing teeth. Despite both new and retained teeth being reduced, Bmp6 OE led to a decrease in the new:retained tooth ratio (*P*=4.4e-5), indicating that exogenous Bmp6 did overall inhibit the tooth replacement rate by more strongly decreasing the number of new teeth present relative to retained teeth. Given that we found a drop in both new and retained teeth, Bmp6 OE necessarily caused a drop in total tooth number (*P*=2.8e-5), resulting in the treatment group having only ~50-60% of the number of teeth that their WT control siblings possessed at the end of the OE treatment. Most of these trends are reflected by each tooth field type alone (Fig S4). Qualitatively, we found large swaths of

stickleback tooth fields that were devoid of erupted teeth (Fig. 5, dotted oval), which was unique to this treatment condition.

We additionally performed a negative control assay on the Bmp6 OE line, again allowing us to ascertain whether carrying the transgene without heat shocks is sufficient to alter any aspects of tooth turnover, total tooth number, and in this case, the tooth "stalling" we uniquely observed under Bmp6 OE. As with the *Wnt10a* negative control experiment, we selected full siblings to the Bmp6 OE treatment animals, and pulse-chased them with no heat shocks in the same containers as our heat shock treatments. We again found no significant deviation in any variable between either pair of groups (Fig. S5). Notably, we found no calcein negative tooth germs in this negative control experiment. In this case, the variance in the non-WT groups did not appear to be increased relative to WT.

We next asked if *bmp6* OE had any of these same effects on zebrafish tooth fields (Fig. 6D). While we did not observe any stalled tooth germs as we did in sticklebacks, we did find a significant decrease in the number of new teeth that formed during the treatment interval (P=0.0042), consistent with a negative role in tooth germ initiation and/or differentiation. Unlike sticklebacks, zebrafish exhibited an increase in retained tooth number (P=0.78). The new:retained ratio, resulting from both an increase in new and decrease in retained, also fell significantly (P=0.013). We did not observe any changes to the number of tooth families present (n=9/9). However, we did detect a significant decrease in the overall number of teeth (P=0.0035), likely brought on by the paucity of new bell stage tooth germs in the OE condition.

To test whether BMP pathway inhibition could promote tooth turnover, we performed an overexpression experiment using the BMP antagonist Grem2a in sticklebacks (Fig. 7A). Grem2a OE did not significantly increase new tooth number (P=0.64) but did decrease retained tooth number (P=0.039). This drop in the retained tooth number per fish was sufficient to increase the new:retained tooth ratio (P=0.029), achieving a higher relative proportion of new

teeth by eliminating retained teeth. However, unlike *Bmp6*, which also decreased the number of retained teeth, Grem2a OE did not significantly reduce total teeth (*P*=0.15). These results are also generally reflected by each tooth field type alone (Fig. S6).

We finally tested *grem2a* OE in zebrafish to ask whether the BMP signaling inhibition also promoted tooth replacement in this species (Fig. 7B-D). This treatment resulted in an increase in the new:retained tooth ratio (*P*=0.00013), which arose from a simultaneous increase of new teeth (*P*=0.00031) and a drop in retained teeth (*P*=0.0047). Zebrafish *grem2a* OE did not alter the number of tooth families observed (n=11/11), nor did it cause a significant change in the total number of teeth (*P*=0.14).

Discussion

Endogenous expression domains of stickleback *Wnt10a, Dkk2, Bmp6,* and *Grem2a* reflect similar germ layer partitioning as in hair follicle gene expression.

We first used *in situ* hybridization to analyze the endogenous expression patterns of *Wnt10a*, *Dkk2*, *Bmp6*, and *Grem2a* in subadult stickleback tooth fields. Our use of sticklebacks allows for a detailed analysis of tooth germ differentiation using only 3-5 individuals per gene, as each subadult stickleback individual (~25 mm standard length) presents ~30+ tooth germs in total. By comparing gene expression between stickleback tooth germs of different observed stages we infer a general tooth organ staging series for each gene, which we can use to interpret whether any expression domains are likely cyclic during the tooth regeneration cycle. As a hair regeneration model would predict, *Wnt10a*, *Dkk2*, *Bmp6*, and *Grem2a* exhibit expression in tooth epithelium and tooth mesenchyme that appears somehow cyclic during tooth organ regeneration. These four genes additionally show expression partitioning between epithelial and

mesenchymal germ layers in ways that overall resemble expression of the mammalian orthologs of these genes in hair follicles (detailed below).

Wnt10a was focally expressed in both epithelium and mesenchyme of developing tooth germs, but epithelial expression appeared to wane by late bell stages, and mesenchymal expression was essentially absent in erupted tooth mesenchyme (Fig. 1A-D). This expression roughly corresponds to the cycle previously observed in the mouse hair follicle, where *Wnt10a* expression was found in the early anagen (growth) phase, but not telogen (the quiescent resting phase which ends with hair shedding)[63]. The Wnt inhibitor *Dkk2* is thought to confer a feedback response in mouse hair follicles, wherein its expression in hair follicle mesenchyme (the dermal papilla) is brought on by Wnt effectors and helps trigger the end of the growth (anagen) phase[52]. Stickleback mesenchymal expression domains of *Wnt10a* and *Dkk2* are generally consistent with such a relationship: *Wnt10a* shows marked expression at the beginning of tooth differentiation (bud stage) that wanes throughout differentiation (Fig. 1A-D, whereas *Dkk2* is excluded from bud stage mesenchymal cells, transcribed during bell stages, and is then highly expressed during and after eruption, especially in fully differentiated apical tooth mesenchyme (odontoblasts; Fig. 1E and F).

BMP pathway genes additionally show expression domains in stickleback tooth fields that are partitioned by germ layer and stage in a way that roughly corresponds to mouse hair follicles. *Bmp6* is highly expressed during growth (anagen) stages of the mouse hair follicle cycle[44], similarly to the inner dental epithelial and mesenchymal expression that is present during early tooth germ growth[42,54] (Fig. 1H). Despite this marked expression of *Bmp6* during organ differentiation, hair follicles have been shown to be delayed from initiating organ development by inhibiting the telogen to anagen transition[44]. Broad similarities exist with teeth: in both stickleback and zebrafish, *Bmp6* demonstrates marked upregulation in specific dental tissues during tooth organ differentiation[42], while also preventing the formation of new tooth

organs (Fig. 6A and D). *Grem2* expression has not been analyzed in mouse hair to our knowledge, but *GREM2* expression in human hair follicles is sharply restricted to the mesenchymal dermal sheath cup, which has led to hypotheses that it regulates the hair follicle stem cell niche[46,64]. Similar to human *GREM2*, stickleback *Grem2a* expression was more widespread in mesenchymal cells in general, however was also more widely expressed than in human hair fields (Fig. 1K-M), including expression in mid-bell stage tooth epithelium and mesenchyme (Fig. 2L), as well as the SDE (Fig. 2M).

Overall, we found that the dental mesenchyme and inner dental epithelium of bell stage tooth germs expresses all four of these secreted ligands. Previous results in sticklebacks and other vertebrate species have described additional expression patterns of an array of Wnt and BMP ligands, inhibitors, and receptors in and around teeth and tooth fields[39,42,54,65–79]. The apparently high representation of different secreted ligands suggests that tooth fields are subject to a rich amalgam of Wnt and BMP signaling molecules overall. It is thus likely that the final output of Wnt or BMP signaling in a given cell might ultimately be regulated by dozens of different secreted ligands and inhibitors all dynamically competing in the extracellular space within the tooth field[80]. The endogenous expression patterns of these secreted factors in tooth fields additionally leaves open the possibility that they participate in some form of reaction-diffusion system between tooth organs and/or more broadly as part of some type of regulatory centers or waves that can coordinate tooth regeneration. Both reaction-diffusion and regulatory wave mechanisms have been hypothesized to explain different coordinated aspects of hair field growth or regeneration[26,81–84]. Intriguingly, some studies have even found specific roles for Wnt and BMP signals in these mechanisms, including *Dkk2*[26,81]. Nevertheless, the four genes we focused on here are all expressed both in tooth germs themselves, as well as in some epithelial and mesenchymal domains that are outside of differentiating or functional tooth organs (Fig. 1, brackets). Any of these expression domains, including those in the “intertooth spaces,” may

work to influence tooth regeneration or total tooth number. Loss of function studies for *Wnt10a*, *Dkk2*, *Bmp6*, and *Grem2a*, including future tissue-specific ablation (e.g. in tooth germs vs. intertooth space) could help determine whether these genes are required for tooth field morphogenesis or regeneration.

Opposing roles of the Wnt and BMP pathways in epithelial appendage regeneration

Wnt and BMP signals have well-documented roles in attenuating hair regeneration in mice. The progression of mouse hair regeneration has been shown to be promoted by Wnt ligands and BMP inhibitors, while inhibited by BMP ligands and Wnt inhibitors[26,43–45,50,85]. This Wnt-BMP oppositional mechanism regulates the cyclic regeneration of hair organs. We reasoned that different epithelial appendages, including teeth, could use a similar basic input scheme to dictate the progression of regeneration, overall being positively influenced by Wnt, and negatively influenced by BMP. To test the hypothesis that teeth and hair share instructive functions for specific secreted ligands during regeneration, we used a candidate gene approach to ask whether specific Wnt and BMP pathway members could regulate tooth regeneration rates in a manner congruent with their known or suspected roles in the Wnt-BMP mechanism described in hair follicles. We thus developed a genetic overexpression (OE) system that could test whether *Wnt10a*, *Dkk2*, *Bmp6*, and *Grem2a* were sufficient to regulate tooth regeneration and/or tooth number overall. To access this in OE treatments on adult and sub-adult organisms actively undergoing tooth regeneration, we measured the number of “new” and “retained” teeth in each fish, calculated a replacement rate of teeth via the new:retained tooth ratio, and also calculated a total tooth number. Our hypothesis specifically predicted that Wnt pathway stimulation or BMP pathway inhibition would increase the replacement rate of teeth, while BMP pathway stimulation or Wnt pathway inhibition would inhibit regeneration. Overall, our results were consistent with our hypothesis: we found that *Wnt10a* or *Grem2a* OE increased tooth

replacement rates in both sticklebacks and zebrafish, while *Bmp6* or *Dkk2* OE both decreased the initiation of new teeth, the former in both sticklebacks and zebrafish, the latter in sticklebacks only (we did not test zebrafish *dkk2* OE). Our overall interpretation of these results is that tooth regeneration is indeed modulated in a congruent fashion as hair with respect to the known, opposing roles of the Wnt and BMP pathways in hair regeneration. Combined with our previous study showing a common genetic battery marks hair follicle stem cells and naïve successional dental epithelia (SDE)[42], these data support a model where teeth and hair, as epithelial appendages, share evolutionarily conserved genetic instructions used to regulate whole organ regeneration. Future and ongoing work will detail the genetic responses to these overexpression treatments to ask whether the genes responding to these different OE conditions also show overlap with hair regeneration.

Regeneration rate and total tooth number can be influenced separately or in concert

Zebrafish typically end primary expansion of their tooth fields at around 30 days old, forming a consistent arrangement of tooth families that is maintained into adulthood[62]. In all three of our zebrafish OE experiments, the replacement rate changed significantly, but the number of tooth families was not significantly altered. Thus, the changes in zebrafish total tooth number we observed (which includes tooth germs) were likely reflecting the higher (*wnt10a*) or lower (*bmp6*) number of tooth families that were actively undergoing regeneration or slowing shedding, causing there to be two ossified teeth at a different number of tooth positions. Conversely, zebrafish *grem2a* OE increased the replacement rate by both increasing new teeth and decreasing retained teeth, without changing the number of tooth families or significantly increasing total tooth number. Overall, these data suggest that zebrafish, like sticklebacks, are capable of measurably adjusting tooth replacement rates without demonstrating significant changes to tooth family number or total tooth number.

Secreted signals that simply promote or inhibit the differentiation of all tooth germs – replacement and primary – would be instead predicted to change the replacement rate while also inhibiting any normal increases to total tooth number in concert. We found that *Dkk2* OE in stickleback best fit the predicted phenotype of a secreted protein that inhibits all tooth formation: new teeth, the replacement rate, and total teeth all dropped under *Dkk2* OE, while retained teeth rose, indicating that tooth turnover and primary growth were both precipitously slowed (Fig. 4A). Notably, *Dkk2* OE appears to have allowed bell stage tooth germs that were present at the time of OE onset to finish development (since zero early, mid- or late bell stage tooth germs were observed in OE fish). Conversely, no zebrafish treatment altered the number of tooth families visible, thus no treatment we performed here was able to affect primary tooth field expansion or contraction in adult zebrafish.

Bmp6 and *Grem2a* OE in sticklebacks both caused a drop in retained tooth number that was not accompanied by an increase in new tooth number. These results strongly suggest that tooth shedding events can be promoted in the absence of increased new tooth formation in sticklebacks. Particularly in the *Bmp6* treatment, tooth shedding increased in the face of a sharp reduction in new teeth. Thus, in sticklebacks, the process of tooth replacement can apparently be regulated not just by influencing the start of replacement tooth formation, but also by independently regulating tooth shedding. These data further support the hypothesis[42,86] that the documented evolutionary changes to tooth number and replacement rate could manifest by changes to tooth shedding mechanics in addition to the tooth formation process.

Other differences and similarities between sticklebacks and zebrafish

Each of our OE treatments affected some aspect of tooth regeneration in a direction predicted by a hair regeneration model. However, the specific nature of each response was not always the same between sticklebacks and zebrafish for the three gene ortholog pairs we tested in both species (*Wnt10*, *Bmp6*, and *Grem2a*). Importantly, the lack of an effect in one species vs the

other could simply reflect limitations of our OE assay: for example, the genomic integration of the OE construct in one species could feasibly be at a genomic location that allows for stronger or weaker transgene expression upon heat shock, causing us to observe unique effects. It is also possible that species-specific protein sequence differences contribute to the differences we observed. Despite these limitations of our approach, we are still able to deduce important similarities and likely differences in how these two animals respond to the overexpression of Wnt and BMP pathway members.

In both species, new teeth were increased by *Wnt10a* OE and decreased by *Bmp6* OE, suggesting that each of these secreted factors exert conserved effects between species that are opposite in their influence on the initiation of replacement tooth growth. *Grem2a*, while it did work to increase the new:retained ratio in both species, achieved this by unique means: in sticklebacks, by only reducing the number of retained teeth (Fig. 7A), and in zebrafish by simultaneously reducing the number of retained teeth and increasing the number of new teeth (Fig. 7B). Grem2a thus may exert some effects in zebrafish that are not realized in sticklebacks, but it remains possible that this secreted factor is activated by shared machinery in hair and teeth, generally facilitating organ replacement.

In zebrafish, significant changes in the tooth replacement rate (as measured by the new:retained ratio) were always at least partly driven by corresponding changes to the number of new teeth. Furthermore, zebrafish retained tooth numbers showed either no detectable change (*wnt10a* and *bmp6*) or changed in the opposite direction as new teeth (*grem2a*). Sticklebacks, on the other hand, showed changes in the replacement rate that were driven either just by changes in retained tooth number (*Grem2a*; Fig. 7A) or where both retained teeth and new teeth changed in the same direction (both decreased under *Bmp6;* Fig. 6A). Thus, sticklebacks twice exhibited the ability to change retained tooth number in a manner that was unlikely a response to the increased generation of new teeth (because new teeth did not

increase), whereas zebrafish never demonstrated this phenomenon. These differences in response between sticklebacks and zebrafish could be partly due to the differences in regeneration strategy exhibited by these fish species: zebrafish adults maintain a set number (11) of stationary tooth families per tooth field that undergo one-for-one replacement in morphologically separated cycles[62], whereas sticklebacks have hundreds of teeth that do not retain a consistent arrangement into adulthood and appear to occasionally engage in one-for-two tooth replacement events[42]. We speculate that the highly canalized tooth regeneration process in zebrafish might contribute to there being less flexibility in the timing of tooth shedding during replacement tooth growth than in a species like stickleback.

Methods

Overexpression transgene constructs

We used restriction-ligation cloning per standard methods to create the heat-shock overexpression construct plasmid backbone used in all seven OE treatments described here. We digested the pT2He-eGFP plasmid with SfiI and BglII, discarded the smaller insert, and ligated the annealed oligos AGGCCCCTAAGGACTAGTCATATGTCTAGACTCGAGCCTAGGGGCGCGCCGGATCCA and GATCTGGATCCGGCGCGCCCCTAGGCTCGAGTCTAGACATATGACTAGTCCTTAGGGGCC TATC onto the ends. This created a plasmid with a multiple cloning site between the forward and reverse Tol2 transposase recognition sequences, including AscI, AvaI, AvrII, BamHI, BglII DraII, SpeI, XbaI, and XhoI restriction enzyme cut sites. We named this intermediate plasmid "T2Rv10." Next, we added the SV40 poly adenylation signal by amplifying it from the pT2He-eGFP reporter construct with the primers GCCGAGATCTCGATGATCCAGACATGATAAG and GTTGTTGAATTCCCATACCACATTTGTAGAG and ligated into T2Rv10 via restriction cloning with BglII and EcoRI. Thereafter we used the primers

ATAGGCCAGATAGGCCTCAGGGGTGTCGCTTGG and AATTGACTAGTCTTGTACAGCTCGTCCATGC to amplify the zebrafish *hsp70l* promoter and the *mCherry* coding sequence (without the stop codon) in tandem from the pT2He-mCherry reporter construct and ligated the product into the plasmid via the SfiI and SpeI restriction sites. Finally, we used the primers AATTGACTAGTGGCAGCGGTGCCACC and GCCGTCTAGAGGGTCCGGGGTTCTCTTC to amplify the Porcine 2A (P2A) self-cleaving peptide coding sequence from the pMS48 plasmid and ligated it into the plasmid via restriction cloning with SpeI and XbaI, yielding the "pT2overCherry" construct used in this work. This plasmid was thereafter outfitted with coding sequences of interest (with a stop codon) downstream of the P2A coding region by using standard restriction site cloning with any two of the AscI, AvrII, BamHI, BglII, XbaI, or XhoI recognition sites that remain available in the multiple cloning site.

Seven coding regions for gene overexpression were synthesized by Gene Universal (Delaware, USA): stickleback *Wnt10a*, *Dkk2, Bmp6*, and *Grem2a*, and zebrafish *wnt10a*, *bmp6*, and *gem2a* (see Table S2 for accession numbers and full DNA sequences). These products were synthesized and cloned into pBlueScript SkII+ by Gene Universal, using XbaI and XhoI restriction enzyme recognition sites in all cases save stickleback *Wnt10a*, for which XbaI and BamHI were used due to an internal cut site for XhoI. Upon receiving these synthesized products, we digested the plasmids using the same restriction enzyme pair that was used to place them into pBlueScript and ligated them into pT2overCherry (digested with the corresponding restriction enzymes and the small insert removed). Ligation products were transformed per standard methods. Colony PCR screening was then performed to identify colonies carrying likely successful ligation products. These were miniprepped (Qiagen) and their full inserts were Sanger sequence verified, leaving ~1 mL of bacterial culture at 4° C to later inoculate a larger liquid culture for midiprep. Once verified, midipreps (Qiagen),

phenol:chloroform extractions, and DNA precipitation was performed per standard methods to prepare plasmids for injection.

Fish husbandry and transgenic line establishment

Zebrafish and stickleback broodstock were raised and maintained under standard conditions. Transgenesis was accomplished by injecting Tol2 mRNA and pT2overCherry plasmids containing the aforementioned coding regions (see Table S2). F0 injected fish were outcrossed to WTs, founders were identified, and a single F1 offspring was thereafter used to establish a stable line from each founder. If the F2 generation exhibited significantly more than 50% transgenic offspring, we outcrossed the line to WT until we observed ~50% transgenic offspring (eliminating insertions until we inferred there was only a single insertion). The work presented here makes use of a single insertion of each transgene for each OE treatment.

Heat shock treatments and pulse-chase bone labeling

To initiate an OE experiment, groups of ~15-20 sibling fish were selected for treatment based on transgene carrier status. We inferred transgene carrier status by lightly sedating fish in 50 mg/mL MS-222 and briefly observing their lenses, where the zebrafish *hsp70l* heat shock promoter drives sustained expression even in the absence of heat shock. WT and OE sibling fish we analyzed were always raised together in a common tank for their entire lives, and only separated briefly from each other during this sorting process. To initiate the treatment, groups of fish were placed into a tank containing a previously described[86] Alizarin Red live-staining solution (0.1 g/L Alizarin Red S with 1mM HEPES) made using either stickleback or zebrafish tank/system water for each species. Sticklebacks were pulsed with Alizarin Red for 24-30 hours in 2L of solution, zebrafish were pulsed for 48-54 hours in 1L of solution (we note that 24 hours in Alizarin Red is insufficient to consistently stain retained teeth 18 days later in zebrafish). Sticklebacks were withheld from food during the Alizarin Red pulse, while zebrafish were fed a

small amount of flake food on the morning of the 2nd day while still in the Alizarin Red solution. After the Alizarin Red staining pulse was completed, the fish were rinsed once then washed 3 times for 10-30 minutes each in fresh tank/system water before being placed into the heat shock tank. Stickleback heat shock tanks were 4L in volume, were lightly aerated with an air stone for increased water agitation (to more uniformly distribute the temperature throughout the tank) and featured two 50 watt aquarium heaters set to 29° Celsius controlled by a timer. The timer engaged the heaters twice per day for two hours per pulse, starting every 12 hours. Since it takes the 4L tanks approximately 50 minutes to ramp up to the heat shock temperature, the two hours of applied heat translates to about 70 minutes at the heat shock temperature per heat shock. Water changes were performed as needed every ~5 days, avoiding the heat shock intervals. Stickleback negative control assays were carried out in exactly the same manner, except the heaters were removed from the 4L "treatment" tank. Zebrafish heat shock tanks essentially followed a published protocol[60], with some modification. Standard 2.8L Aquaneering tanks with a single 50W tank heater set to 39° C were kept on either a dripping water flow rate or with no flow, and were not aerated (normal zebrafish movement was sufficient to agitate the water and create a uniform temperature throughout the tank). The timer activated the heater twice per day for 90 minutes, starting every 12 hours. Since it takes ~2.8L of zebrafish system water about 20 minutes to heat to 39° C, these treatments brought fish to the heat shock temperature for around 70 minutes per treatment, as in the stickleback heat shock treatments. Water changes were performed at least once every four days by turning the tank flow on high for 10+ minutes, again avoiding the heat shock intervals. After the 36th heat shock on the 18th day of the treatment, both species of fish were withheld from feeding, removed from their respective heat shock tanks, and live stained in a calcien live staining solution[86] (0.05 g/L calcein with 1mM sodium phosphate) for 16-18 hours, in 2L for sticklebacks and 1L for zebrafish. After rinsing and washing the fish in their corresponding tank/system water at least

three times over 30 min, fish were euthanized in 250 mg/mL MS-222, sorted by red channel fluorescence, and fixed in 4% PFA overnight at 4° C with high agitation.

Preparation and blinding of pulse-chase labeled tooth fields

Following fixation, fish from OE experiments were rinsed and washed in tap water, then agitated in 1% KOH for 20+ minutes at room temperature. Dental tissues were dissected out in system water or 1X PBS, then washed at room temperature with 1% KOH overnight or with 5% KOH for 30-60 minutes, rendering the mCherry signal no longer detectable. Dental tissues were then washed through a glycerol series (25, 50, 90% glycerol in 1x PBS). Stickleback pharyngeal tissues were flat mounted as previously described[87], while zebrafish pharyngeal tooth fields and stickleback oral jaws were arrayed into 24 well plates. The resulting pule-chase dental samples were then shuffled and renamed irrespective of treatment condition so that a different researcher could blindly score and count the teeth in each dental preparation (i.e. the researcher scoring the teeth did not prepare the dissected tooth fields nor did they know which individuals carried an OE transgene).

Scoring and analyzing pulse-chase assays

Dental preparations were scored on a Leica M165 stereomicroscope using GFP2, strict GFP, and Rhodamine filters to observe Alizarin Red and calcein staining. Every tooth in each animal was addressed for both species (left and right premaxillary, dentary, DTP1, DTP2, and VTP tooth fields in sticklebacks, and the VTP in zebrafish). Importantly, we find that the pulse-chase signal is markedly more difficult to interpret after ~1 week at room temperature or ~3 weeks stored at 4° C, both because the calcein signal fades and because autofluorescence in soft tissues increases. Skeletal preparations from a given experiment were thus always scored within two days of the end of each experiment, and always within a single 24 hour window. Since actively growing bony tooth tissues (dentine and enameloid) strongly incorporate these

stains, this pulse-chase strategy allows us to classify each tooth in each individual as either "new" or "retained" with respect to the treatment interval: "new" teeth are those that began bone deposition after the Alizarin Red pulse (during the OE treatment), and are thus only marked by the 2nd stain, calcein, while "retained" teeth are those that show any Alizarin Red stain, because this indicates that these teeth were depositing bone prior to the treatment interval (see Fig. 2F-H). The only exception to these rules was in the stickleback Bmp6 OE treatment, where tooth germs in the treatment condition were observed without either stain. Because these tooth germs were Alizarin Red negative, we inferred that these were new teeth despite their lack of calcein stain; i.e. we interpret that this class of tooth germs had halted bone deposition by the time the calcein chase occurred. The new:retained ratio and total tooth number for each fish was additionally calculated by dividing or summing new and retained counts, respectively. We additionally counted morphological tooth families in each zebrafish specimen to address primary tooth number expansion or contraction in this species. All statistical tests were performed in R, using two-sided Wilcoxon rank-sum tests in all cases. After scoring was complete, example pulse-chase sample examples were imaged on a Leica DM2500 compound microscope, Leica M165 stereomicroscope, or Zeiss LSM 700 confocal microscope.

In situ hybridization

In situ hybridization on sections from subadult and adult sticklebacks was performed as previously described[42]. See Table S1 for probe template sequence information. Probes designed to *Wnt10a* and *Bmp6* were published previously[42,54]. A 3' UTR probe template for *Grem2a* was cloned from genomic DNA via PCR using the primers GGTGCAGAGGGTCAAACAGT and ATACAGGCTCGTGTCCAAGC. The probe template for *Dkk2* was created from the purchased full-length coding sequence (Gene Universal, Delaware, USA) that was also used to create the overexpression construct (described above). Digoxygenin-labeled *in situ* riboprobes were synthesized as previously described[42]. WT material

was embedded in paraffin and sectioned as previously described on either the sagittal or coronal plane[42].

Hematoxylin and Eosin staining

Dkk2 OE and sibling WT fish underwent a typical OE treatment but were not pulsed or chased with Alizarin Red or calcein. These fish were then fixed and sorted as described above. Thereafter these fish were decapitated, and their heads were prepared for sectioning on the coronal plane a previously described[42]. Sections were stained with Hematoxylin and Eosin as previously described[42].

Acknowledgements

We thank Andrew Glazer for cloning the stickleback *Grem2a* riboprobe template, Tess Linden and Nicole King for sharing the pMS48 plasmid, Mark Stepaniak for creating and sharing the T2Rv10 plasmid, and Sophie Archambeault and Naama Weksler for feedback on the manuscript. This work was supported by NIH grants DE027871, DE031017, and DE021475.

Figure legends

Figure 1. *In situ* hybridization detects dynamic expression of *Wnt10a*, *Dkk2*, *Bmp6*, and *Grem2a* within and surrounding pharyngeal tooth organs in subadult wild-type sticklebacks. The basalmost layer of epithelium is flanked by black dotted lines in each image. Arrows mark dental epithelium, arrowheads mark dental mesenchyme, black pointers mark detected expression, white markers indicate regions with no detected expression, brackets mark mesenchymal expression outside of tooth organs, and carets mark the successional dental epithelium. **A-D.** *Wnt10a* transcripts were detected focally in bud stage tooth germs (A), in both epithelium (black arrow) and mesenchyme (black arrowhead). In mid-bell stage tooth germs (B), expression was detected in the inner dental epithelium (black arrow) and tooth mesenchyme (black arrowhead).

In late bell (D) and eruption stage teeth (C), epithelial expression was no longer detected (white arrows), but mesenchymal expression persists (black arrowheads). In fully ankylosed and erupted teeth (C and D), *Wnt10a* expression was not widely detected. *Wnt10a* expression was additionally detected in localized mesenchymal cells surrounding tooth organs (bracket in A). **E and F.** *Dkk2* transcripts diffusely mark pharyngeal dental epithelium (upper portion of both images), including early bud stage tooth germs (left black arrow in E), but are not detected in bud stage mesenchyme (white arrowhead in E). Epithelial transcripts were most strongly detected in mid-bell stage inner dental epithelium (right black arrow in E), and mid-bell mesenchyme (black arrowhead in E). Expression is additionally detected in mesenchymal clusters near the bone of attachment (bracket in E). Expression in tooth mesenchyme is additionally detected in fully ankylosed erupted teeth (black arrowhead in F). **G-J.** *Bmp6* transcripts were detected in bud stage tooth epithelium and mesenchyme (black arrow and arrowhead in G), bell stage inner dental epithelium and mesenchyme (black arrow and arrowhead in H). *Bmp6* was not detected in eruption stage tooth epithelium (white arrow in I) but was detected in eruption stage mesenchyme (black arrowhead in I) and erupted tooth mesenchyme (black arrowhead in J). *Bmp6* was also transcribed in some successional dental epithelia (caret in I). Localized mesenchymal expression between teeth was also detected (brackets in I). **K-M**. *Grem2a* transcripts were not detected in bud stage tooth germ epithelium or mesenchyme (white arrow and arrowhead in K). Bell stage tooth germs and eruption stage teeth exhibited expression in inner and outer dental epithelium (black arrows in L and M). Tooth mesenchyme was *Grem2a* positive in bell stages through fully ankylosed, erupted teeth (black arrowheads in L and M). *Grem2a* was additionally detected in mesenchyme surrounding tooth organs (brackets in K and M) and in the successional dental epithelium (caret in M). Scale bars: 20 μm.

Figure 2. Summary of the two-stain pulse-chase heat shock method for assessing tooth gain and loss. **A.** A schematic of the transgene used. The zebrafish *hsp70l* promoter drives the expression of an mCherry-P2A-CDS transgene, where "CDS" is one of seven full length coding sequences of interest (see Methods and Table S2). P2A (Porcine 2A) is a 22 amino acid sequence that has been shown to self-cleave on translation between residues 20 and 21. This separates mCherry from the CDS, leaving the bulk of the P2A protein on the C terminus of mCherry. **B.** Example temperature profiles for heat shock treatments. Alizarin pulse and calcein chase are shown as pink and green bars, respectively. **C.** Lateral images of sticklebacks 24 hours after a single heat shock. Control (WT) on top, overexpression transgene positive (OE) fish on bottom (*Bmp6* OE in this example). C' shows red channel fluorescence, allowing us to visualize the transcription of our overexpression transgene. **D and E.** Dissecting the ventral tooth plate (VTP) from each WT and OE fish reveals mCherry localized to the tooth field itself (E' shows red channel fluorescence). Anterior to top. **F.** Example images of the pulse-chase method on a control individual. Alizarin Red (F) strongly marks all bone undergoing active ossification at the start of the treatment (false colored pink). **F'.** 18 days later, after 36 heat shocks, a calcein chase marks all bone ossifying at the end of the treatment (green). **F''.** Overlain images of stickleback pharyngeal teeth showing Alizarin Red and calcein reveals whether individual teeth were either present at only the 2nd labeling (new, calcein only, example marked "n") or if they were present at both the first and the second labeling (retained, Alizarin Red and calcein positive, example marked "r"). **G.** An overlay of the pulse-chase treatment on zebrafish teeth using the same treatment interval (see panel B, zebrafish example).

Figure 3. Effects of *Wnt10a* overexpression in stickleback and zebrafish. **A.** In sticklebacks, the number of new teeth (P=0.00072), retained teeth (P=0.010), and the new:retained ratio (P=0.0003) showed significant differences between WT and OE fish, however the total number of teeth did not (P=0.81). **B and C.** Overlay images of stickleback ventral tooth plates showing

Alizarin Red and calcein signal in control (B) and OE (C) individuals. Note clusters of new teeth (white dotted circle showing an example on the left VTP). **D.** In zebrafish, significant increases in the number of new teeth (*P*=0.00039), the new:retained ratio (*P*=0.0042), and total teeth (*P*=0.011) were found but retained tooth number (*P*=0.56) did not significantly change.

Figure 4. Effects of *Dkk2* overexpression in stickleback. **A.** Significant decreases in the number of new teeth (*P*=0.00024), the new:retained ratio (*P*=1.1e-5), and total teeth (*P*=0.0036) were detected, while an increase in retained teeth (*P*=0.045) was observed. **B and C.** Overlay images of stickleback ventral tooth plates showing Alizarin Red and calcein signal in control (B) and OE (C) individuals. Note near complete absence of unankylosed new teeth in the OE individual (white arrow in C) compared to the WT individual (white arrows in B). The right side is left unlabeled. **D and E.** Hematoxylin and Eosin (H&E) staining reveals no tooth germs of any stage in *Dkk2* OE fish (n=7/7), suggesting that this treatment does not cause tooth germs to arrest (yellow ovals in D show tooth germs, asterisks in E sit above positions normally populated by tooth germs).

Figure 5. Stalled tooth germs resulting from the Bmp6 overexpression treatment. A shows WT control, B shows OE transgene carrier. A and B show brightfield, A’ and B’ show green channel fluorescence (calcein), A’’ and B’’ show an overlay. Note that there is no caclein signal in the four tooth germs indicated in the Bmp6 OE individual (gray arrows in B’). Black and white arrows otherwise mark tooth germs in those panels where they are visible.

Figure 6. Effects of Bmp6 overexpression in stickleback and zebrafish. **A.** In sticklebacks, significant decreases in all four variables were detected: the number of new teeth (*P*=2.7e-5), the number of retained teeth (*P*=2.8e-5), the new:retained ratio (*P*=4.4e-5), and total teeth (*P*=2.8e-5). **B and C.** Overlay images of stickleback ventral tooth plates showing Alizarin Red and calcein signal in control (B) and OE (C) individuals. Note regions usually populated with ankylosed teeth are completely devoid of any such structure (dotted oval in D, the right side is

left unlabeled). **D.** In zebrafish, significant decreases in the number of new teeth (*P*=0.0042), the new:retained ratio (*P*=0.013), and total teeth (*P*=0.0035) were detected but retained tooth number (*P*=0.78) did not significantly change.

Figure 7. Effects of Grem2a overexpression in stickleback and zebrafish. **A.** In sticklebacks, significant decrease in the number of retained teeth (*P*=0.039), a significant increase in the new:retained ratio (*P*=0.029), but no significant changes to new teeth (*P*=0.64) or total teeth (*P*=0.15) were observed. **B.** In zebrafish, significant increases in the number of new teeth (*P*=0.00031), and the new:retained ratio (*P*=0.00013) were found, and a significant decrease in retained teeth (*P*=0.0047), however no significant change in total teeth (*P*=0.14) was observed. **C and D.** Overlay images of zebrafish ventral tooth plates showing Alizarin Red and calcein signal in control (B) and OE (C) individuals. White circles indicate new teeth, solid circles mark those that are superficial, dotted circles mark those that are deep in the tooth field and thus occluded by erupted teeth.

Figure S1. Results of stickleback *Wnt10a* OE parsed by tooth field. Stickleback pharyngeal teeth are housed in three discrete fields: the 1st dorsal tooth plate 1 (DTP1), the 2nd dorsal tooth plate (DTP2), and the ventral tooth plate (VTP). In the oral jaws, sticklebacks have teeth on their premaxilla (Premax) and dentary (Dent) bones. Each group of graphs shows new, retained, the new:retained ratio, and total tooth number broken down by tooth field type (the sum of left and right halves per fish).

Figure S2. Negative control experiment with *Wnt10a* transgene carriers. The same pulse-chase interval (18 days, see Methods) with no heat shocks was applied to full siblings of the individuals in the experiment summarized in Fig. 3A, testing for whether simply carrying the transgene in the absence of any heat shock is associated with changes in the number of new teeth, retained teeth, the new:retained ratio, or total teeth; no such deviations were detected in this negative control experiment for any of these four variables assessed (all *P*>0.68).

Figure S3. Results of stickleback *Dkk2* OE parsed by tooth field. Stickleback pharyngeal teeth are housed in three discrete fields: the 1st dorsal tooth plate 1 (DTP1), the 2nd dorsal tooth plate (DTP2), and the ventral tooth plate (VTP). In the oral jaws, sticklebacks have teeth on their premaxilla (Premax) and dentary (Dent) bones. Each group of graphs shows new, retained, the new:retained ratio, and total tooth number broken down by tooth field type (the sum of left and right halves per fish).

Figure S4. Results of stickleback Bmp6 OE parsed by tooth field. Stickleback pharyngeal teeth are housed in three discrete fields: the 1st dorsal tooth plate 1 (DTP1), the 2nd dorsal tooth plate (DTP2), and the ventral tooth plate (VTP). In the oral jaws, sticklebacks have teeth on their premaxilla (Premax) and dentary (Dent) bones. Each group of graphs shows new, retained, the new:retained ratio, and total tooth number broken down by tooth field type (the sum of left and right halves per fish).

Figure S5. Negative control experiment with *Bmp6* transgene carriers. The same pulse-chase interval (18 days, see Methods) with no heat shocks was applied to full siblings of the individuals in the experiment summarized in Fig. 6A, testing for whether simply carrying the transgene in the absence of any heat shock is associated with changes in the number of new teeth, retained teeth, the new:retained ratio, or total teeth; no such deviations were detected in this negative control experiment for any of these four variables assessed (all $P>0.26$). Additionally, no “stalled” tooth germs were observed.

Figure S6. Results of stickleback Bmp6 OE parsed by tooth field. Stickleback pharyngeal teeth are housed in three discrete fields: the 1st dorsal tooth plate 1 (DTP1), the 2nd dorsal tooth plate (DTP2), and the ventral tooth plate (VTP). In the oral jaws, sticklebacks have teeth on their premaxilla (Premax) and dentary (Dent) bones. Each group of graphs shows new, retained, the new:retained ratio, and total tooth number broken down by tooth field type (the sum of left and right halves per fish).

References cited

1. Tucker AS, Fraser GJ. Evolution and developmental diversity of tooth regeneration. *Seminars in Cell & Developmental Biology*. 2014;25-26:71-80. doi:10.1016/j.semcdb.2013.12.013
2. Whitlock JA, Richman JM. Biology of tooth replacement in amniotes. *Int J Oral Sci*. 2013;5(2):66-70. doi:10.1038/ijos.2013.36
3. Sire JY, Davit-Beal T, Delgado S, Van Der Heyden C, Huysseune A. First-generation teeth in nonmammalian lineages: Evidence for a conserved ancestral character? *Microscopy Research and Technique*. 2002;59(5):408-434. doi:10.1002/jemt.10220
4. Grieco TM, Richman JM. Coordination of bilateral tooth replacement in the juvenile gecko is continuous with in ovo patterning. *Evol Dev*. 2018;20(2):51-64. doi:10.1111/ede.12247
5. Osborn JW. New Approach to Zahnreihen. *Nature*. 1970;225(5230):343-346. doi:10.1038/225343a0
6. Osborn JW. Relationship between growth and the pattern of tooth initiation in alligator embryos. *J Dent Res*. 1998;77(9):1730-1738. doi:10.1177/00220345980770090901
7. DeMar R. Evolutionary Implications of Zahnreihen. *Evolution*. 1972;26(3):435-450. doi:10.2307/2407018
8. Edmund AG. *Tooth Replacement Phenomena in the Lower Vertebrates*. [Toronto]□: Royal Ontario Museum; 1960. Accessed September 30, 2022. http://archive.org/details/toothreplacement00edmu
9. Fraser G, Thiery A. Evolution, Development, and Regeneration of Fish Dentitions. Cambridge University Press 978-1-107-17944-8 -Evolution and Development of Fishes. In: ; 2020.
10. Yuan Q, Zhao M, Tandon B, Maili L, Liu X, Zhang A, Baugh EH, Tran T, Silva RM, Hecht JT, Swindell EC, Wagner DS, Letra A. Role of WNT10A in failure of tooth development in humans and zebrafish. *Molecular Genetics & Genomic Medicine*. 2017;5(6):730-741. doi:10.1002/mgg3.332
11. Xu M, Horrell J, Snitow M, Cui J, Gochnauer H, Syrett CM, Kallish S, Seykora JT, Liu F, Gaillard D, Katz JP, Kaestner KH, Levin B, Mansfield C, Douglas JE, Cowart BJ, Tordoff M, Liu F, Zhu X, Barlow LA, Rubin AI, McGrath JA, Morrisey EE, Chu EY, Millar SE. WNT10A mutation causes ectodermal dysplasia by impairing progenitor cell proliferation and KLF4-mediated differentiation. *Nature Communications*. 2017;8(1):15397. doi:10.1038/ncomms15397
12. Jia S, Kwon HJE, Lan Y, Zhou J, Liu H, Jiang R. Bmp4-Msx1 signaling and Osr2 control tooth organogenesis through antagonistic regulation of secreted Wnt antagonists. *Developmental Biology*. 2016;420(1):110-119. doi:10.1016/j.ydbio.2016.10.001
13. Hu X, Wang Y, He F, Li L, Zheng Y, Zhang Y, Chen YP. Noggin is required for early development of murine upper incisors. *J Dent Res*. 2012;91(4):394-400. doi:10.1177/0022034511435939
14. Vogel P, Liu J, Platt KA, Read RW, Thiel M, Vance RB, Brommage R. Malformation of incisor teeth in Grem2$^{-/-}$ mice. *Vet Pathol*. 2015;52(1):224-229. doi:10.1177/0300985814528218
15. Seppala M, Fraser GJ, Birjandi AA, Xavier GM, Cobourne MT. Sonic Hedgehog Signaling and Development of the Dentition. *J Dev Biol*. 2017;5(2):6. doi:10.3390/jdb5020006
16. Gibert Y, Samarut E, Ellis MK, Jackman WR, Laudet V. The first formed tooth serves as a signalling centre to induce the formation of the dental row in zebrafish. *Proceedings of the Royal Society B: Biological Sciences*. 2019;286(1904):20190401. doi:10.1098/rspb.2019.0401
17. Jackman WR, Draper BW, Stock DW. Fgf signaling is required for zebrafish tooth development. *Developmental Biology*. 2004;274(1):139-157. doi:10.1016/j.ydbio.2004.07.003
18. Harris MP, Rohner N, Schwarz H, Perathoner S, Konstantinidis P, Nüsslein-Volhard C. Zebrafish eda and edar Mutants Reveal Conserved and Ancestral Roles of Ectodysplasin Signaling in Vertebrates. *PLOS Genetics*. 2008;4(10):e1000206. doi:10.1371/journal.pgen.1000206
19. Aigler SR, Jandzik D, Hatta K, Uesugi K, Stock DW. Selection and constraint underlie irreversibility of tooth loss in cypriniform fishes. *PNAS*. 2014;111(21):7707-7712. doi:10.1073/pnas.1321171111
20. Jandzik D, Stock DW. Differences in developmental potential predict the contrasting patterns of dental diversification in characiform and cypriniform fishes. *Proceedings of the Royal Society B: Biological Sciences*. 2021;288(1944):20202205. doi:10.1098/rspb.2020.2205
21. Tucker A, Sharpe P. The cutting-edge of mammalian development; how the embryo makes teeth. *Nature Reviews Genetics*. 2004;5(7):499-508. doi:10.1038/nrg1380
22. Balic A, Thesleff I. Tissue Interactions Regulating Tooth Development and Renewal. *Curr Top Dev Biol*. 2015;115:157-186. doi:10.1016/bs.ctdb.2015.07.006
23. Chuong CM, Noveen A. Phenotypic Determination of Epithelial Appendages: Genes, Developmental Pathways, and Evolution. *Journal of Investigative Dermatology Symposium Proceedings*. 1999;4(3):307-311. doi:10.1038/sj.jidsp.5640235
24. Wu P, Hou L, Plikus M, Hughes M, Scehnet J, Suksaweang S, Widelitz RB, Jiang TX, Chuong CM. Evo-Devo of Amniote Integuments and Appendages. *Int J Dev Biol*. 2004;48(0):249-270. doi:10.1387/ijdb.041825pw
25. Chuong CM, Randall VA, Widelitz RB, Wu P, Jiang TX. Physiological regeneration of skin appendages and implications for regenerative medicine. *Physiology (Bethesda)*. 2012;27(2):61-72. doi:10.1152/physiol.00028.2011
26. Plikus MV, Mayer JA, de la Cruz D, Baker RE, Maini PK, Maxson R, Chuong CM. Cyclic dermal BMP signalling regulates stem cell activation during hair regeneration. *Nature*. 2008;451(7176):340-344. doi:10.1038/nature06457
27. Lin SJ, Wideliz RB, Yue Z, Li A, Wu X, Jiang TX, Wu P, Chuong CM. Feather regeneration as a model for organogenesis. *Dev Growth Differ*. 2013;55(1):139-148. doi:10.1111/dgd.12024

28. Cox BD, De Simone A, Tornini VA, Singh SP, Di Talia S, Poss KD. In Toto Imaging of Dynamic Osteoblast Behaviors in Regenerating Skeletal Bone. *Curr Biol*. 2018;28(24):3937-3947.e4. doi:10.1016/j.cub.2018.10.052
29. Wu P, Alibardi L, Chuong C. Regeneration of reptilian scales after wounding: neogenesis, regional difference, and molecular modules. *Regeneration (Oxf)*. 2014;1(1):15-26. doi:10.1002/reg2.9
30. Finger TE, Barlow LA. Cellular diversity and regeneration in taste buds. *Current Opinion in Physiology*. 2021;20:146-153. doi:10.1016/j.cophys.2021.01.003
31. Rocchi C, Barazzuol L, Coppes RP. The evolving definition of salivary gland stem cells. *npj Regen Med*. 2021;6(1):1-8. doi:10.1038/s41536-020-00115-x
32. Lin Y, Chen L, Zhang M, Xie S, Du L, Zhang X, Li H. Eccrine Sweat Gland and Its Regeneration: Current Status and Future Directions. *Frontiers in Cell and Developmental Biology*. 2021;9. Accessed September 30, 2022. https://www.frontiersin.org/articles/10.3389/fcell.2021.667765
33. Du W, Du W, Yu H. The Role of Fibroblast Growth Factors in Tooth Development and Incisor Renewal. *Stem Cells Int*. 2018;2018:7549160. doi:10.1155/2018/7549160
34. Di-Poï N, Milinkovitch MC. The anatomical placode in reptile scale morphogenesis indicates shared ancestry among skin appendages in amniotes. *Sci Adv*. 2016;2(6). doi:10.1126/sciadv.1600708
35. Debiais-Thibaud M, Oulion S, Bourrat F, Laurenti P, Casane D, Borday-Birraux V. The homology of odontodes in gnathostomes: insights from Dlx gene expression in the dogfish, Scyliorhinus canicula. *BMC Evolutionary Biology*. 2011;11(1):307. doi:10.1186/1471-2148-11-307
36. Pispa J, Thesleff I. Mechanisms of ectodermal organogenesis. *Developmental Biology*. 2003;262(2):195-205. doi:10.1016/S0012-1606(03)00325-7
37. Sharpe PT. Fish scale development: Hair today, teeth and scales yesterday? *Current Biology*. 2001;11(18):R751-R752. doi:10.1016/S0960-9822(01)00438-9
38. Benton MJ, Dhouailly D, Jiang B, McNamara M. The Early Origin of Feathers. *Trends in Ecology & Evolution*. 2019;34(9):856-869. doi:10.1016/j.tree.2019.04.018
39. Rasch LJ, Martin KJ, Cooper RL, Metscher BD, Underwood CJ, Fraser GJ. An ancient dental gene set governs development and continuous regeneration of teeth in sharks. *Developmental Biology*. 2016;415(2):347-370. doi:10.1016/j.ydbio.2016.01.038
40. Martin KJ, Rasch LJ, Cooper RL, Metscher BD, Johanson Z, Fraser GJ. Sox2+ progenitors in sharks link taste development with the evolution of regenerative teeth from denticles. *PNAS*. 2016;113(51):14769-14774. doi:10.1073/pnas.1612354113
41. Aman AJ, Fulbright AN, Parichy DM. Wnt/β-catenin regulates an ancient signaling network during zebrafish scale development. White RM, Stainier DY, eds. *eLife*. 2018;7:e37001. doi:10.7554/eLife.37001
42. Square TA, Sundaram S, Mackey EJ, Miller CT. Distinct tooth regeneration systems deploy a conserved battery of genes. *EvoDevo*. 2021;12(1):4. doi:10.1186/s13227-021-00172-3
43. Kandyba E, Leung Y, Chen YB, Widelitz R, Chuong CM, Kobielak K. Competitive balance of intrabulge BMP/Wnt signaling reveals a robust gene network ruling stem cell homeostasis and cyclic activation. *PNAS*. 2013;110(4):1351-1356. doi:10.1073/pnas.1121312110
44. Wu P, Zhang Y, Xing Y, Xu W, Guo H, Deng F, Ma X, Li Y. The balance of Bmp6 and Wnt10b regulates the telogen-anagen transition of hair follicles. *Cell Communication and Signaling*. 2019;17(1):16. doi:10.1186/s12964-019-0330-x
45. Daszczuk P, Mazurek P, Pieczonka TD, Olczak A, Boryń ŁM, Kobielak K. An Intrinsic Oscillation of Gene Networks Inside Hair Follicle Stem Cells: An Additional Layer That Can Modulate Hair Stem Cell Activities. *Frontiers in Cell and Developmental Biology*. 2020;8. Accessed September 30, 2022. https://www.frontiersin.org/articles/10.3389/fcell.2020.595178
46. Niiyama S, Ishimatsu-Tsuji Y, Kishimoto J. Niche formed by bone morphogenetic protein antagonists gremlin 1 and gremlin 2 in human hair follicles. *Health Sci Rep*. 2022;5(1):e486. doi:10.1002/hsr2.486
47. Botchkarev VA, Botchkareva NV, Nakamura M, Huber O, Funa K, Lauster R, Paus R, Gilchrest BA. Noggin is required for induction of the hair follicle growth phase in postnatal skin. *FASEB J*. 2001;15(12):2205-2214. doi:10.1096/fj.01-0207com
48. Greco V, Chen T, Rendl M, Schober M, Pasolli HA, Stokes N, dela Cruz-Racelis J, Fuchs E. A Two-Step Mechanism for Stem Cell Activation during Hair Regeneration. *Cell Stem Cell*. 2009;4(2):155-169. doi:10.1016/j.stem.2008.12.009
49. Kishimoto J, Burgeson RE, Morgan BA. Wnt signaling maintains the hair-inducing activity of the dermal papilla. *Genes Dev*. 2000;14(10):1181-1185.
50. Rendl M, Polak L, Fuchs E. BMP signaling in dermal papilla cells is required for their hair follicle-inductive properties. *Genes Dev*. 2008;22(4):543-557. doi:10.1101/gad.1614408
51. Kwack MH, Kim MK, Kim JC, Sung YK. Dickkopf 1 Promotes Regression of Hair Follicles. *Journal of Investigative Dermatology*. 2012;132(6):1554-1560. doi:10.1038/jid.2012.24
52. Harshuk-Shabso S, Dressler H, Niehrs C, Aamar E, Enshell-Seijffers D. Fgf and Wnt signaling interaction in the mesenchymal niche regulates the murine hair cycle clock. *Nat Commun*. 2020;11(1):5114. doi:10.1038/s41467-020-18643-x
53. Mostowska A, Biedziak B, Zadurska M, Bogdanowicz A, Olszewska A, Cieślińska K, Firlej E, Jagodziński P. GREM2 nucleotide variants and the risk of tooth agenesis. *Oral Diseases*. 2018;24(4):591-599. doi:10.1111/odi.12793
54. Cleves PA, Ellis NA, Jimenez MT, Nunez SM, Schluter D, Kingsley DM, Miller CT. Evolved tooth gain in sticklebacks is associated with a cis-regulatory allele of Bmp6. *PNAS*. 2014;111(38):13912-13917. doi:10.1073/pnas.1407567111
55. Cleves PA, Hart JC, Agoglia RM, Jimenez MT, Erickson PA, Gai L, Miller CT. An intronic enhancer of Bmp6 underlies evolved tooth gain in sticklebacks. *PLOS Genetics*. 2018;14(6):e1007449. doi:10.1371/journal.pgen.1007449
56. Song Y, Boncompagni AC, Kim SS, Gochnauer HR, Zhang Y, Loots GG, Wu D, Li Y, Xu M, Millar SE. Regional Control of Hairless versus Hair-Bearing Skin by Dkk2. *Cell Rep*. 2018;25(11):2981-2991.e3. doi:10.1016/j.celrep.2018.11.017

57. Hart JC, Ellis NA, Eisen MB, Miller CT. Convergent evolution of gene expression in two high-toothed stickleback populations. *PLOS Genetics*. 2018;14(6):e1007443. doi:10.1371/journal.pgen.1007443
58. Popa EM, Buchtova M, Tucker AS. Revitalising the rudimentary replacement dentition in the mouse. *Development*. 2019;146(3). doi:10.1242/dev.171363
59. Järvinen E, Salazar-Ciudad I, Birchmeier W, Taketo MM, Jernvall J, Thesleff I. Continuous tooth generation in mouse is induced by activated epithelial Wnt/β-catenin signaling. *PNAS*. 2006;103(49):18627-18632. doi:10.1073/pnas.0607289103
60. Duszynski RJ, Topczewski J, LeClair EE. Simple, Economical Heat-Shock Devices for Zebrafish Housing Racks. *Zebrafish*. 2011;8(4):211-219. doi:10.1089/zeb.2011.0693
61. Shoji W, Sato-Maeda M. Application of heat shock promoter in transgenic zebrafish. *Dev Growth Differ*. 2008;50(6):401-406. doi:10.1111/j.1440-169X.2008.01038.x
62. Van der Heyden C, Huysseune A. Dynamics of tooth formation and replacement in the zebrafish (Danio rerio) (Teleostei, Cyprinidae). *Dev Dyn*. 2000;219(4):486-496. doi:10.1002/1097-0177(2000)9999:9999<::AID-DVDY1069>3.0.CO;2-Z
63. Reddy S, Andl T, Bagasra A, Lu MM, Epstein DJ, Morrisey EE, Millar SE. Characterization of Wnt gene expression in developing and postnatal hair follicles and identification of Wnt5a as a target of Sonic hedgehog in hair follicle morphogenesis. *Mechanisms of Development*. 2001;107(1):69-82. doi:10.1016/S0925-4773(01)00452-X
64. Niiyama S, Ishimatsu-Tsuji Y, Nakazawa Y, Yoshida Y, Soma T, Ideta R, Mukai H, Kishimoto J. Gene Expression Profiling of the Intact Dermal Sheath Cup of Human Hair Follicles. *Acta Derm Venereol*. 2018;98(7):694-698. doi:10.2340/00015555-2949
65. Fraser GJ, Graham A, Smith MM. Developmental and evolutionary origins of the vertebrate dentition: molecular controls for spatio-temporal organisation of tooth sites in osteichthyans. *J Exp Zool B Mol Dev Evol*. 2006;306(3):183-203. doi:10.1002/jez.b.21097
66. Fraser GJ, Hulsey CD, Bloomquist RF, Uyesugi K, Manley NR, Streelman JT. An Ancient Gene Network Is Co-opted for Teeth on Old and New Jaws. *PLoS Biol*. 2009;7(2). doi:10.1371/journal.pbio.1000031
67. Fraser GJ, Cerny R, Soukup V, Bronner-Fraser M, Streelman JT. The Odontode Explosion: The origin of tooth-like structures in vertebrates. *Bioessays*. 2010;32(9):808-817. doi:10.1002/bies.200900151
68. Porntaveetus T, Otsuka-Tanaka Y, Albert Basson M, Moon AM, Sharpe PT, Ohazama A. Expression of fibroblast growth factors (Fgfs) in murine tooth development. *J Anat*. 2011;218(5):534-543. doi:10.1111/j.1469-7580.2011.01352.x
69. Fjeld K, Kettunen P, Furmanek T, Kvinnsland IH, Luukko K. Dynamic expression of Wnt signaling-related Dickkopf1, -2, and -3 mRNAs in the developing mouse tooth. *Developmental Dynamics: An Official Publication of the American Association of Anatomists*. 2005;233(1):161-166. doi:10.1002/dvdy.20285
70. Gong AX, Zhang JH, Li J, Wu J, Wang L, Miao DS. Comparison of gene expression profiles between dental pulp and periodontal ligament tissues in humans. *Int J Mol Med*. 2017;40(3):647-660. doi:10.3892/ijmm.2017.3065
71. Krivanek J, Soldatov RA, Kastriti ME, Chontorotzea T, Herdina AN, Petersen J, Szarowska B, Landova M, Matejova VK, Holla LI, Kuchler U, Zdrilic IV, Vijaykumar A, Balic A, Marangoni P, Klein OD, Neves VCM, Yianni V, Sharpe PT, Harkany T, Metscher BD, Bajénoff M, Mina M, Fried K, Kharchenko PV, Adameyko I. Dental cell type atlas reveals stem and differentiated cell types in mouse and human teeth. *Nat Commun*. 2020;11(1):4816. doi:10.1038/s41467-020-18512-7
72. Aberg T, Wozney J, Thesleff I. Expression patterns of bone morphogenetic proteins (Bmps) in the developing mouse tooth suggest roles in morphogenesis and cell differentiation. *Dev Dyn*. 1997;210(4):383-396. doi:10.1002/(SICI)1097-0177(199712)210:4<383::AID-AJA3>3.0.CO;2-C
73. Wang B, Li H, Liu Y, Lin X, Lin Y, Wang Y, Hu X, Zhang Y. Expression patterns of WNT/β-CATENIN signaling molecules during human tooth development. *J Mol Hist*. 2014;45(5):487-496. doi:10.1007/s10735-014-9572-5
74. Wang XP, Suomalainen M, Felszeghy S, Zelarayan LC, Alonso MT, Plikus MV, Maas RL, Chuong CM, Schimmang T, Thesleff I. An Integrated Gene Regulatory Network Controls Stem Cell Proliferation in Teeth. *PLOS Biology*. 2007;5(6):e159. doi:10.1371/journal.pbio.0050159
75. Vainio S, Karavanova I, Jowett A, Thesleff I. Identification of BMP-4 as a signal mediating secondary induction between epithelial and mesenchymal tissues during early tooth development. *Cell*. 1993;75(1):45-58. doi:10.1016/S0092-8674(05)80083-2
76. Sarkar L, Sharpe PT. Expression of Wnt signalling pathway genes during tooth development. *Mech Dev*. 1999;85(1-2):197-200. doi:10.1016/s0925-4773(99)00095-7
77. Suomalainen M, Thesleff I. Patterns of Wnt pathway activity in the mouse incisor indicate absence of Wnt/beta-catenin signaling in the epithelial stem cells. *Dev Dyn*. 2010;239(1):364-372. doi:10.1002/dvdy.22106
78. Luukko K, Løes S, Furmanek T, Fjeld K, Kvinnsland IH, Kettunen P. Identification of a novel putative signaling center, the tertiary enamel knot in the postnatal mouse molar tooth. *Mechanisms of Development*. 2003;120(3):270-276. doi:10.1016/S0925-4773(02)00458-6
79. Huysseune A, Soenens M, Elderweirdt F. Wnt signaling during tooth replacement in zebrafish (Danio rerio): pitfalls and perspectives. *Front Physiol*. 2014;5. doi:10.3389/fphys.2014.00386
80. Mitsiadis TA, Graf D. Cell fate determination during tooth development and regeneration. *Birth Defect Res C*. 2009;87(3):199-211. doi:10.1002/bdrc.20160
81. Sick S, Reinker S, Timmer J, Schlake T. WNT and DKK Determine Hair Follicle Spacing Through a Reaction-Diffusion Mechanism. *Science*. 2006;314(5804):1447-1450. doi:10.1126/science.1130088
82. Plikus MV, Widelitz RB, Maxson R, Chuong CM. Analyses of regenerative wave patterns in adult hair follicle populations reveal macro-environmental regulation of stem cell activity. *Int J Dev Biol*. 2009;53(5-6):857-868. doi:10.1387/ijdb.072564mp

83. Chen CC, Murray PJ, Jiang TX, Plikus MV, Chang YT, Lee OK, Widelitz RB, Chuong CM. Regenerative hair waves in aging mice and extra-follicular modulators Follistatin, Dkk1 and Sfrp4. *J Invest Dermatol*. 2014;134(8):2086-2096. doi:10.1038/jid.2014.139

84. Nagorcka BN. Evidence for a reaction-diffusion system as a mechanism controlling mammalian hair growth. *Biosystems*. 1983;16(3):323-332. doi:10.1016/0303-2647(83)90015-1

85. Kobielak K, Stokes N, Cruz J de la, Polak L, Fuchs E. Loss of a quiescent niche but not follicle stem cells in the absence of bone morphogenetic protein signaling. *PNAS*. 2007;104(24):10063-10068. doi:10.1073/pnas.0703004104

86. Ellis NA, Glazer AM, Donde NN, Cleves PA, Agoglia RM, Miller CT. Distinct developmental genetic mechanisms underlie convergently evolved tooth gain in sticklebacks. *Development*. 2015;142(14):2442-2451. doi:10.1242/dev.124248

87. Ellis NA, Miller CT. Dissection and Flat-mounting of the Threespine Stickleback Branchial Skeleton. *JoVE (Journal of Visualized Experiments)*. 2016;(111):e54056. doi:10.3791/54056

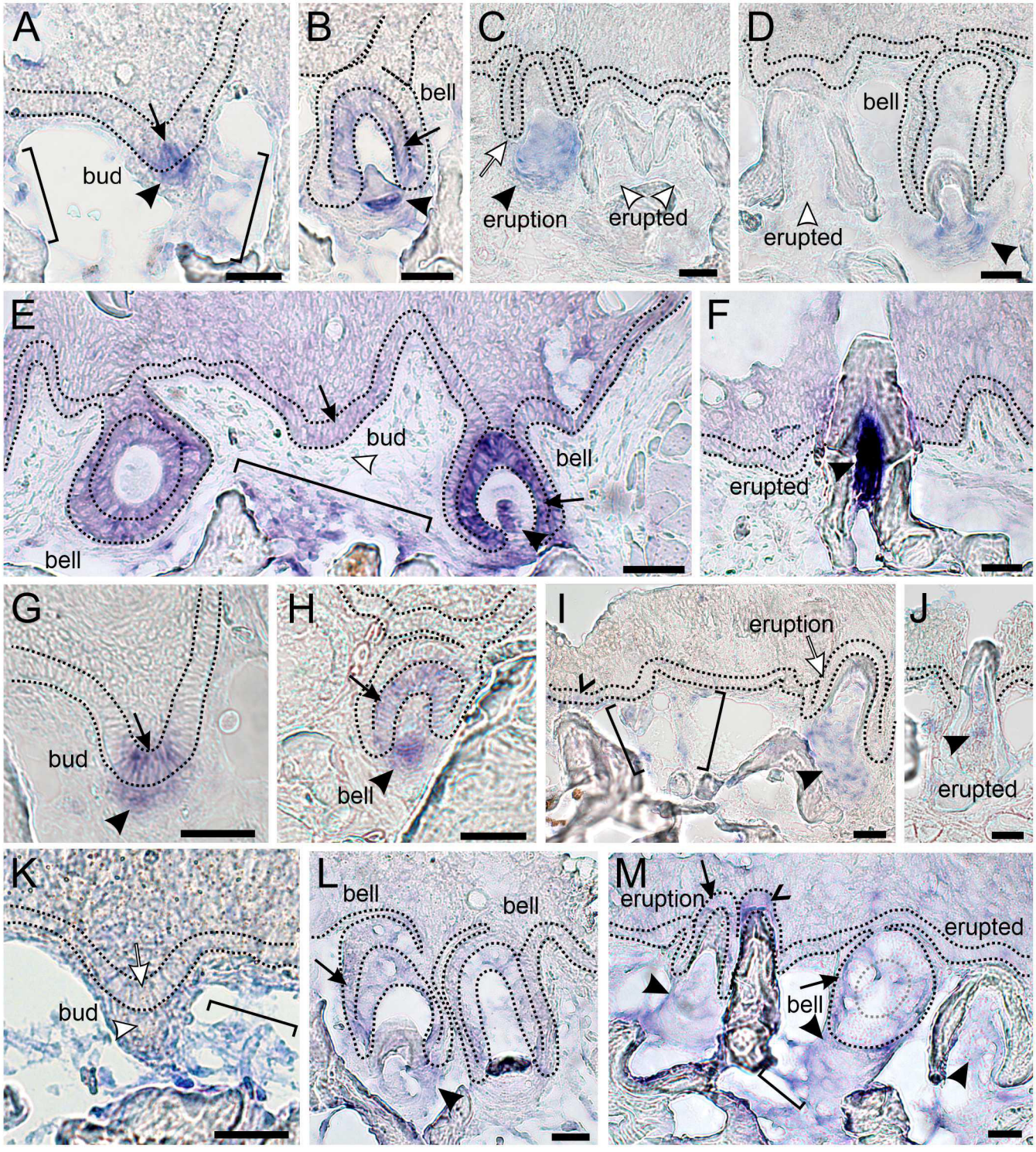
Wnt10a
Dkk2
Bmp6
Grem2a
A
bud
B
bell
C
eruption
erupted
D
bell
erupted
E
bud
bell
bell
F
erupted
G
bud
H
bell
I
eruption
J
erupted
K
bud
L
bell
bell
M
eruption
erupted
bell

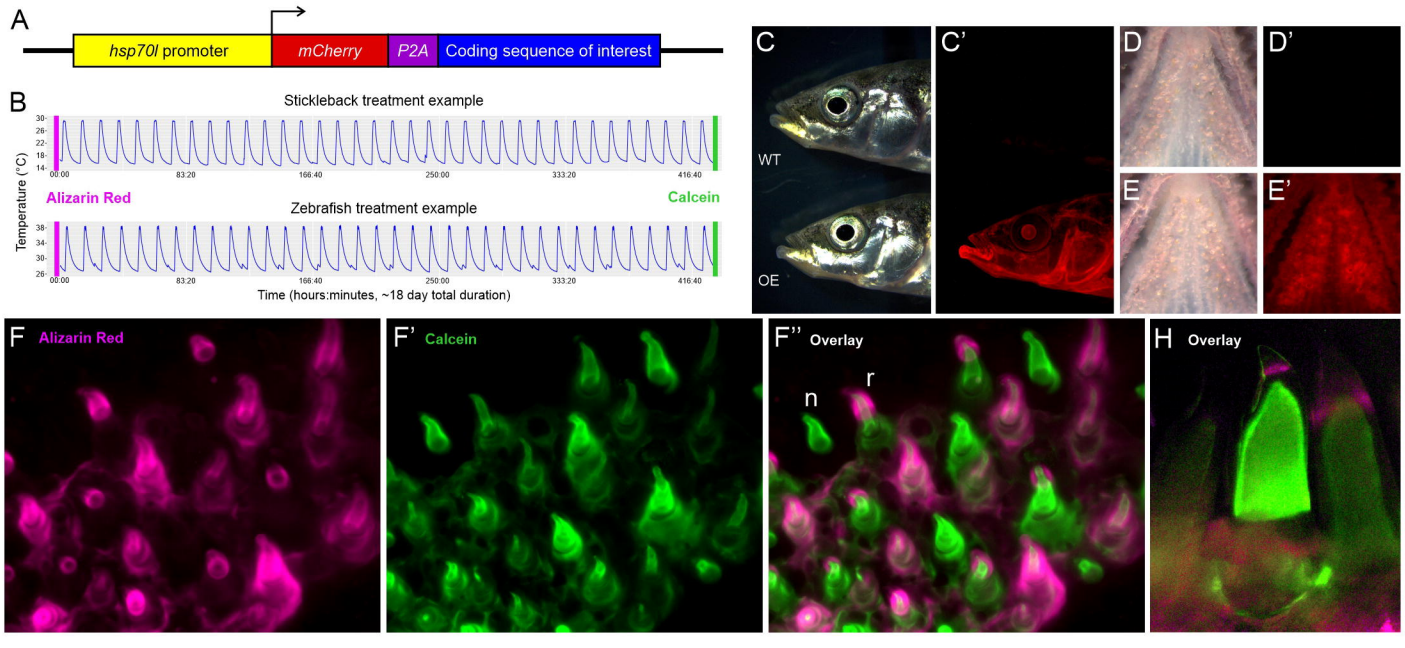
A
hsp70l promoter
mCherry
P2A
Coding sequence of interest
B
Stickleback treatment example
Alizarin Red
Calcein
Zebrafish treatment example
Temperature (°C)
Time (hours:minutes, ~18 day total duration)
C
C'
WT
OE
D
D'
E
E'
F Alizarin Red
F' Calcein
F'' Overlay
n
r
H Overlay

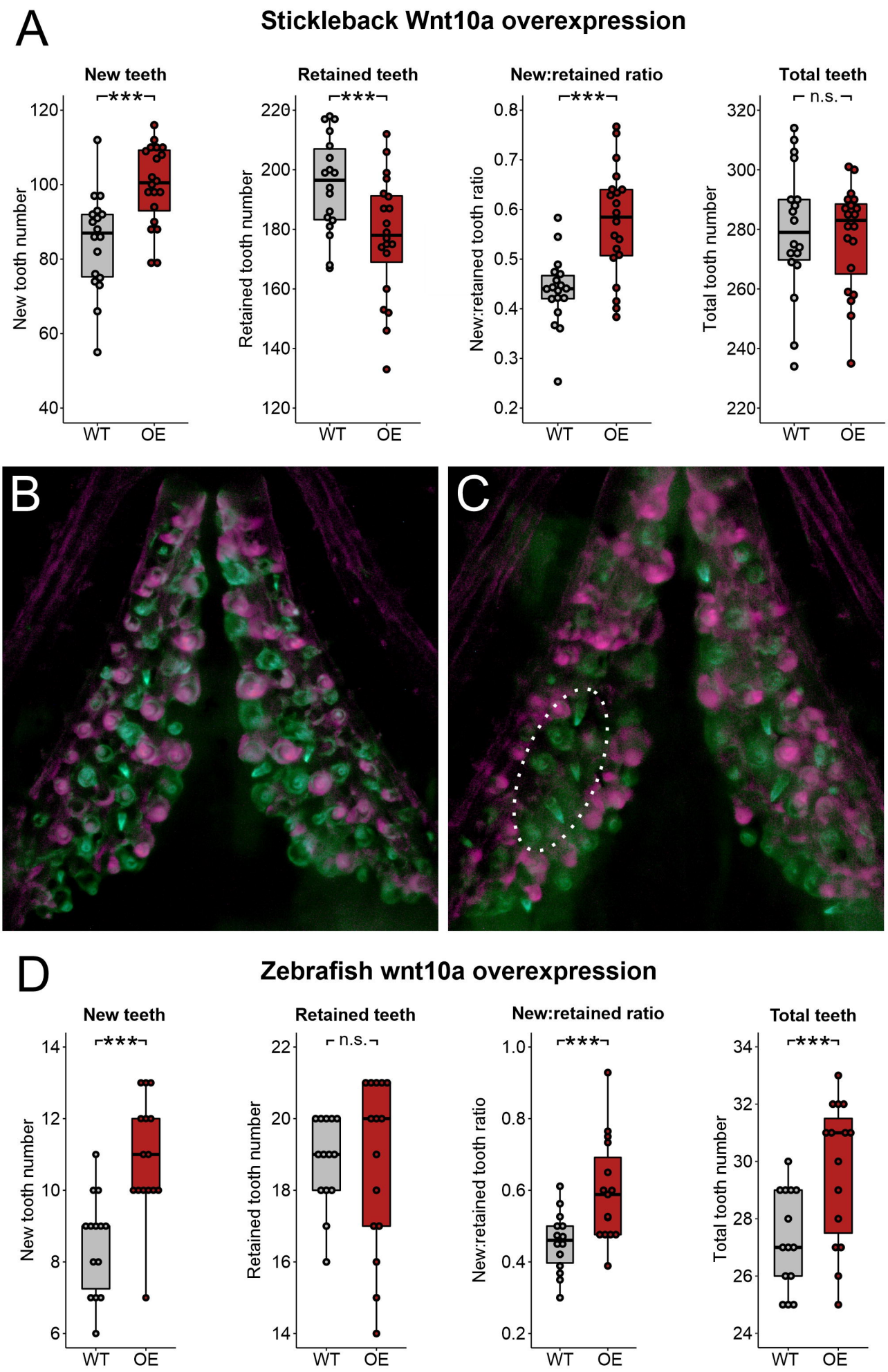

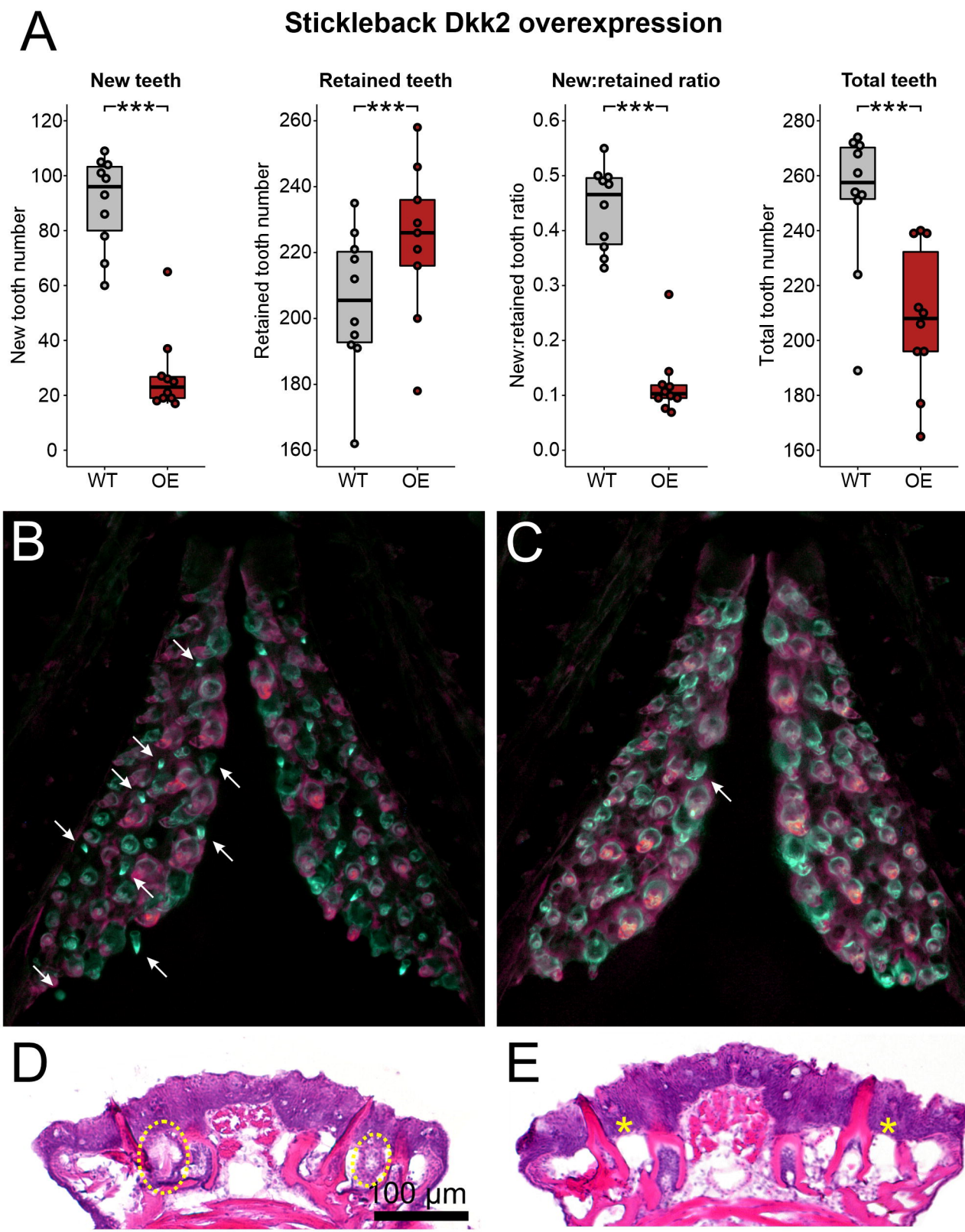
A
Stickleback Dkk2 overexpression
New teeth
***
New tooth number
120
100
80
60
40
20
0
WT
OE
Retained teeth
***
Retained tooth number
260
240
220
200
180
160
WT
OE
New:retained ratio
***
New:retained tooth ratio
0.6
0.5
0.4
0.3
0.2
0.1
0.0
WT
OE
Total teeth
***
Total tooth number
280
260
240
220
200
180
160
WT
OE
B
C
D
100 µm
E
*
*

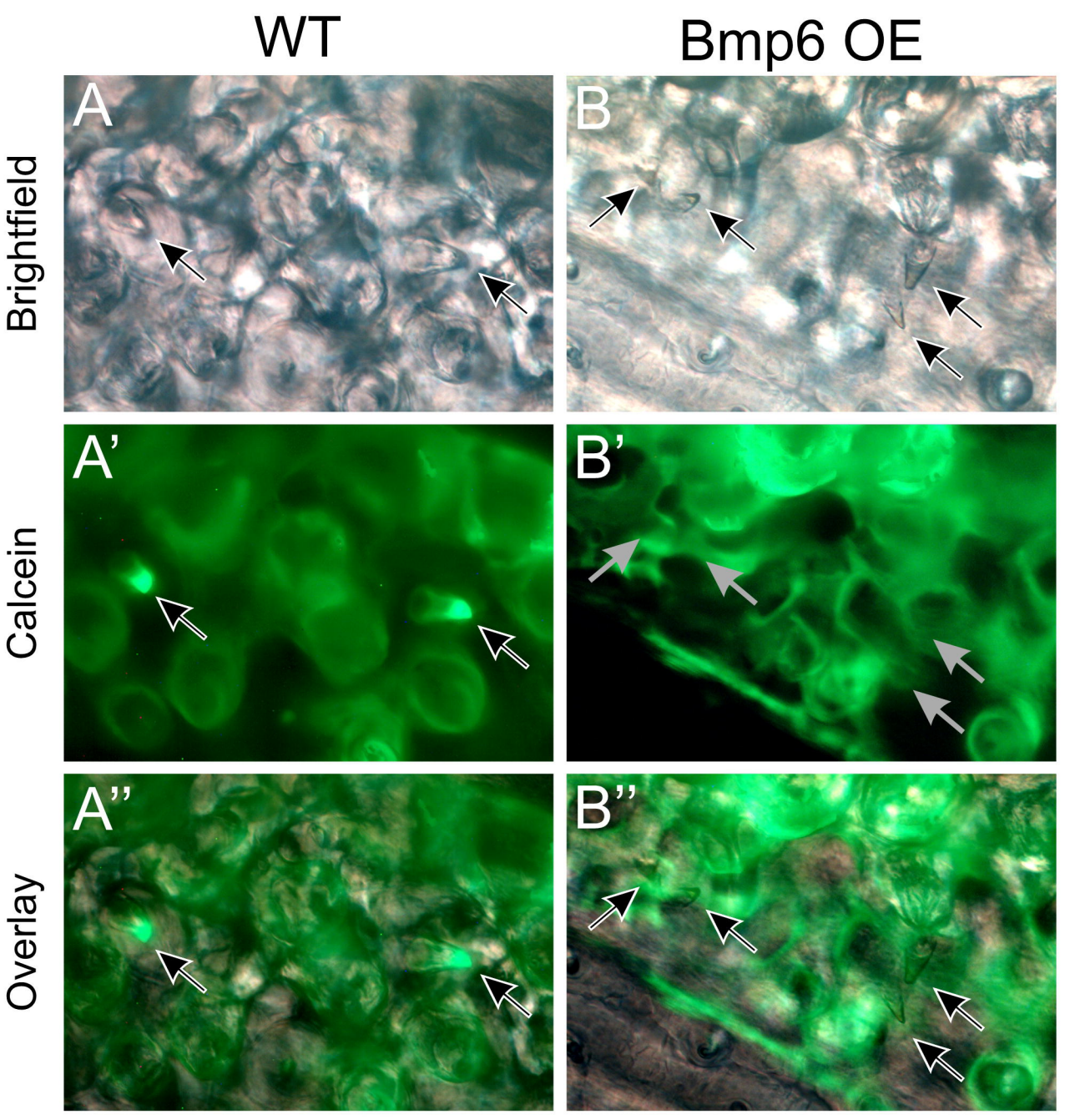
WT
Bmp6 OE
Brightfield
Calcein
Overlay
A
B
A'
B'
A''
B''

A

Stickleback Bmp6 overexpression

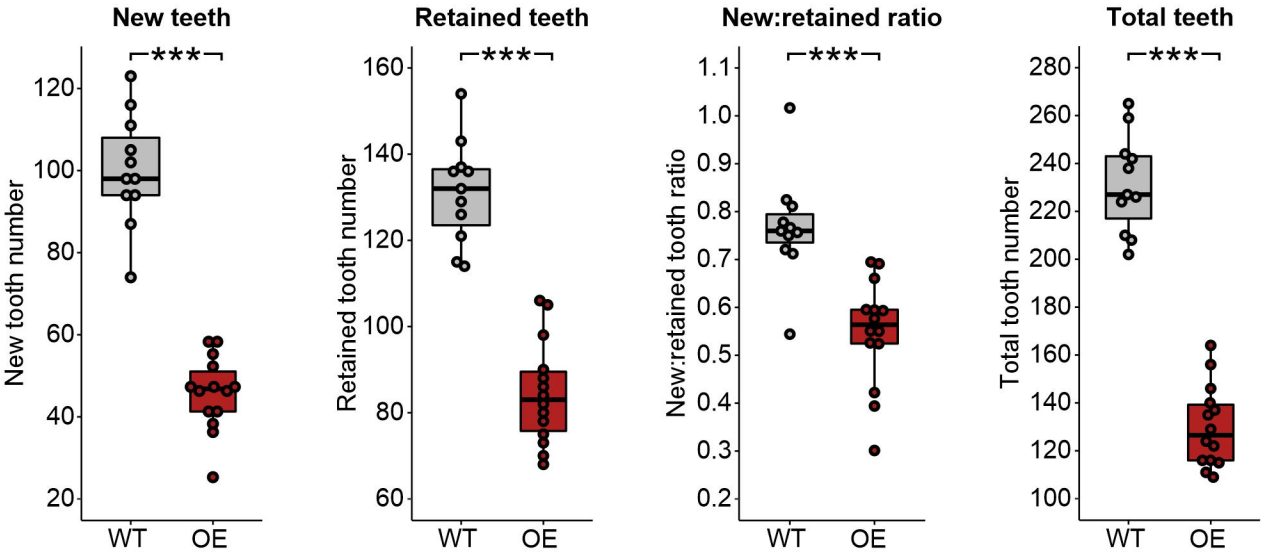

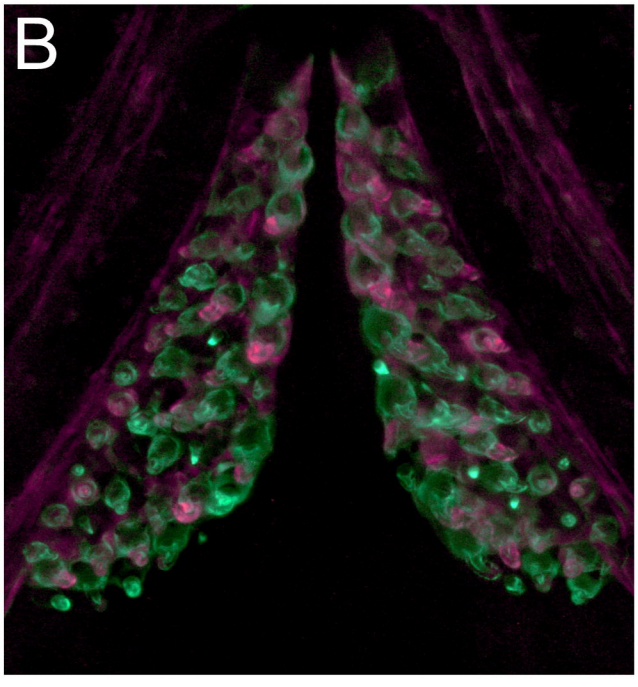

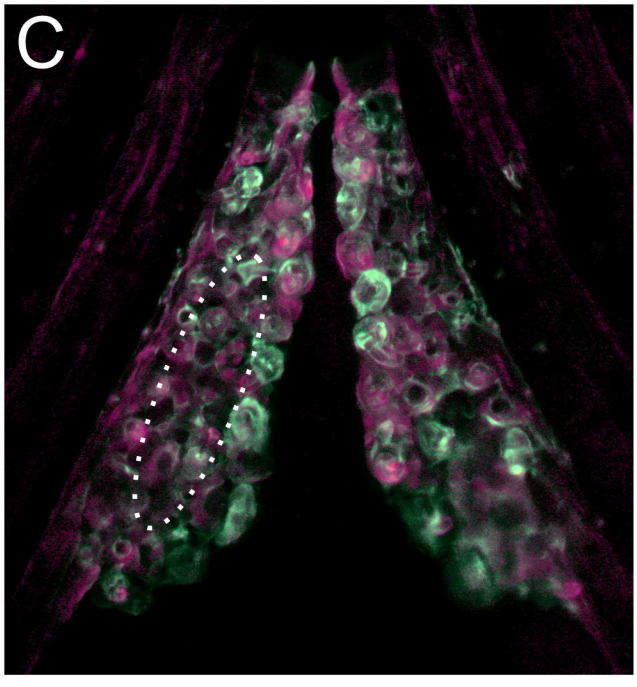

D

Zebrafish bmp6 overexpression

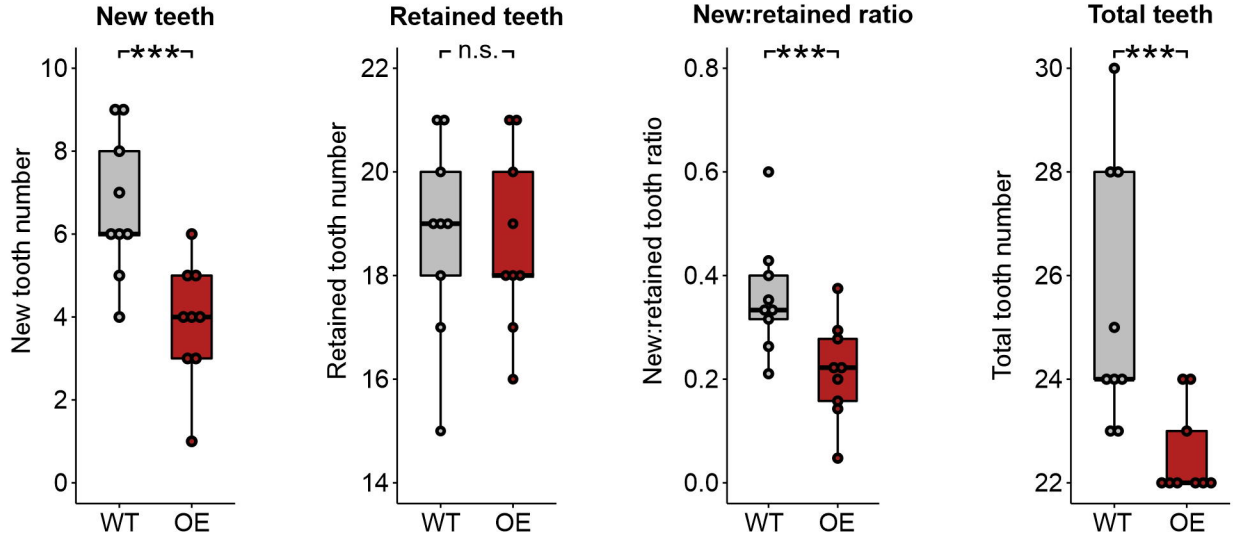

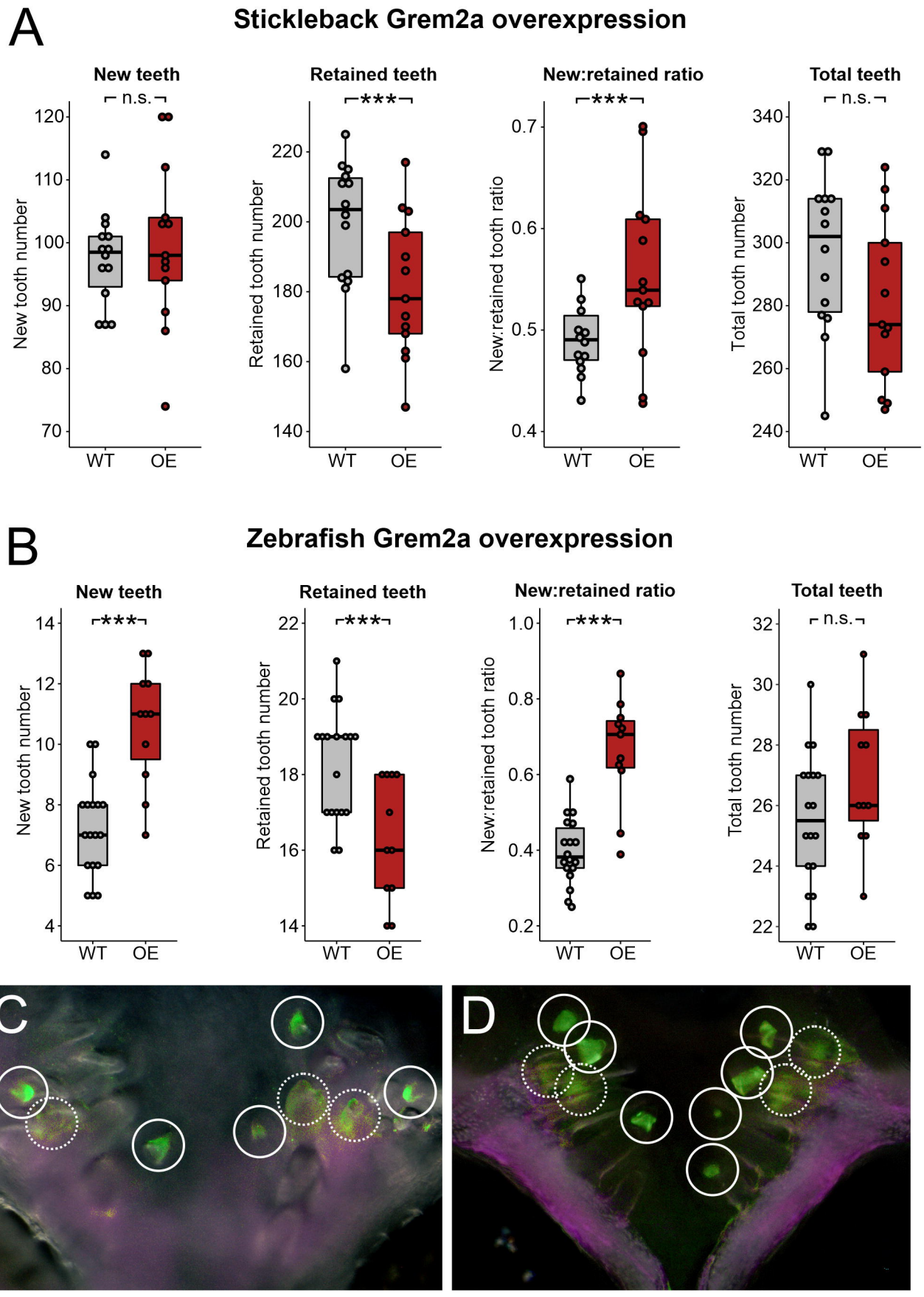
A
Stickleback Grem2a overexpression
New teeth
n.s.
New tooth number
120
110
100
90
80
70
WT
OE
Retained teeth
***
Retained tooth number
220
200
180
160
140
WT
OE
New:retained ratio
***
New:retained tooth ratio
0.7
0.6
0.5
0.4
WT
OE
Total teeth
n.s.
Total tooth number
340
320
300
280
260
240
WT
OE
B
Zebrafish Grem2a overexpression
New teeth
***
New tooth number
14
12
10
8
6
4
WT
OE
Retained teeth
***
Retained tooth number
22
20
18
16
14
WT
OE
New:retained ratio
***
New:retained tooth ratio
1.0
0.8
0.6
0.4
0.2
WT
OE
Total teeth
n.s.
Total tooth number
32
30
28
26
24
22
WT
OE
C
D

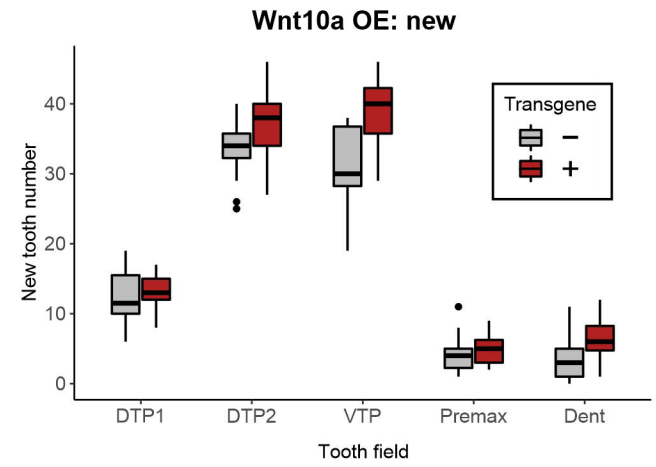
Wnt10a OE: new
New tooth number
Tooth field
DTP1
DTP2
VTP
Premax
Dent
Transgene
−
+

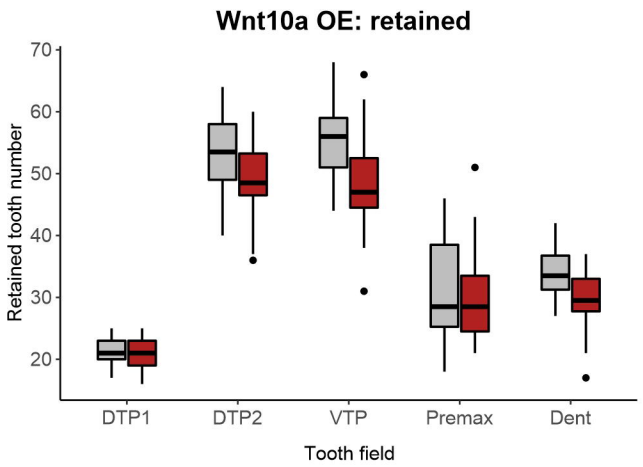
Wnt10a OE: retained
Retained tooth number
Tooth field
DTP1
DTP2
VTP
Premax
Dent

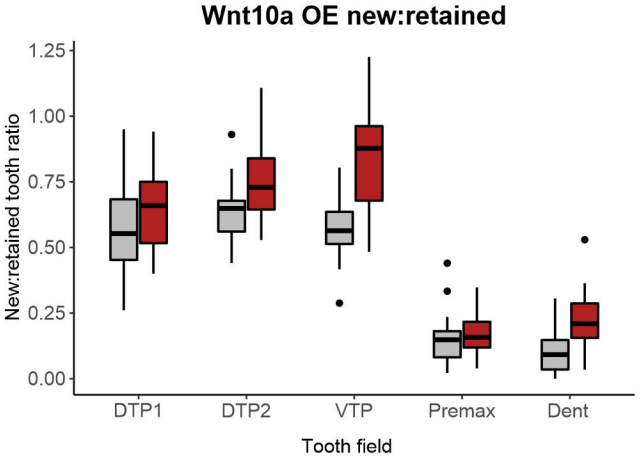
Wnt10a OE new:retained
New:retained tooth ratio
Tooth field
DTP1
DTP2
VTP
Premax
Dent

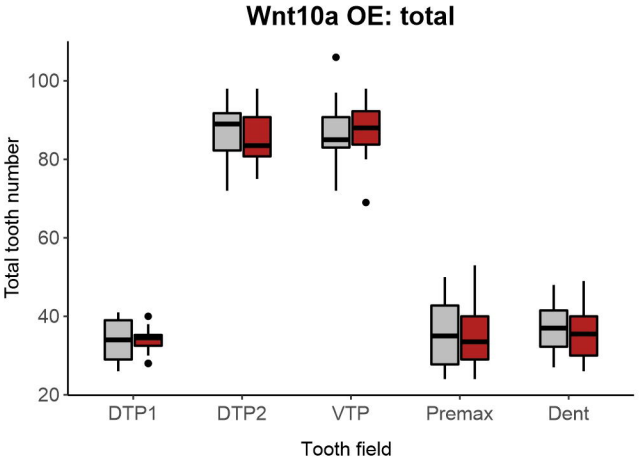
Wnt10a OE: total
Total tooth number
Tooth field
DTP1
DTP2
VTP
Premax
Dent

Stickleback Wnt10a negative control

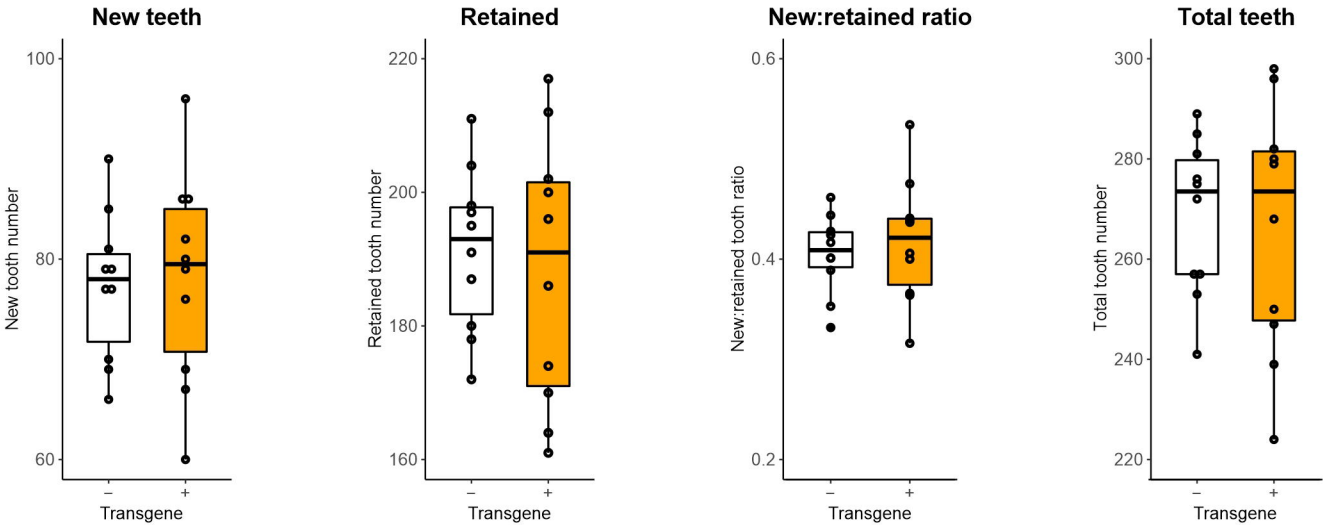

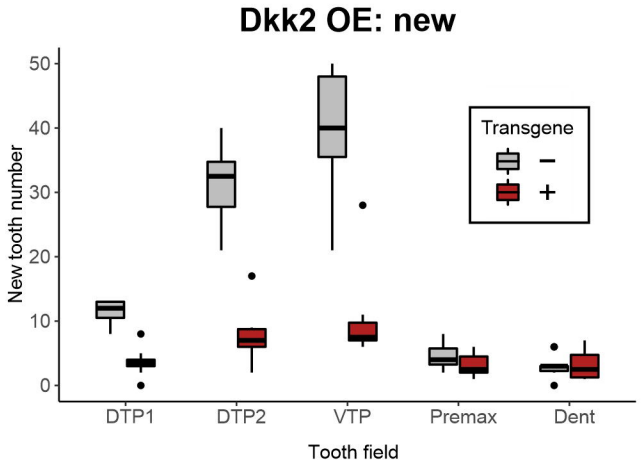
Dkk2 OE: new
New tooth number
50
40
30
20
10
0
Transgene
−
+
DTP1
DTP2
VTP
Premax
Dent
Tooth field

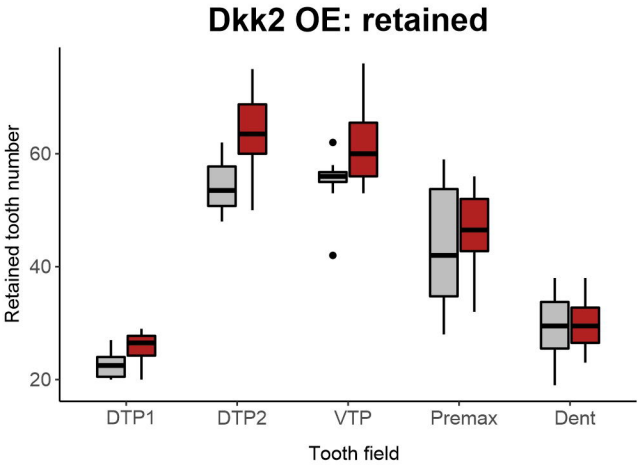
Dkk2 OE: retained
Retained tooth number
60
40
20
DTP1
DTP2
VTP
Premax
Dent
Tooth field

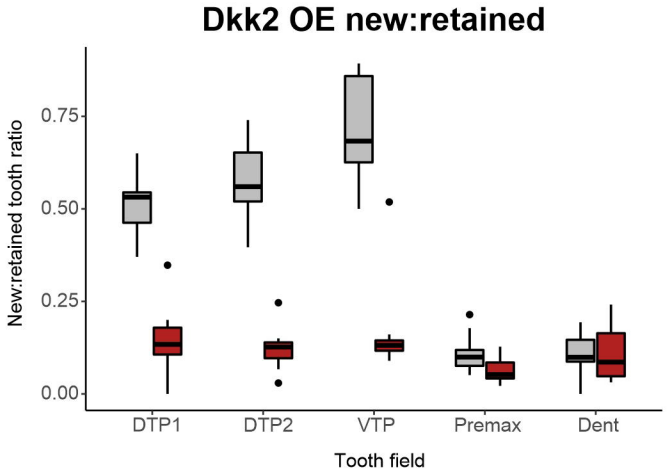
Dkk2 OE new:retained
New:retained tooth ratio
0.75
0.50
0.25
0.00
DTP1
DTP2
VTP
Premax
Dent
Tooth field

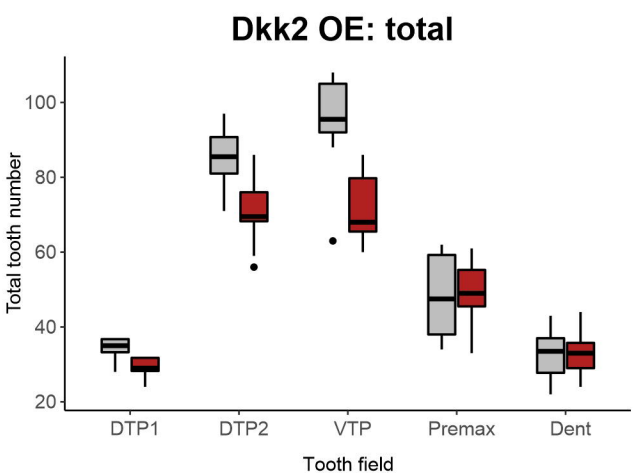
Dkk2 OE: total
Total tooth number
100
80
60
40
20
DTP1
DTP2
VTP
Premax
Dent
Tooth field

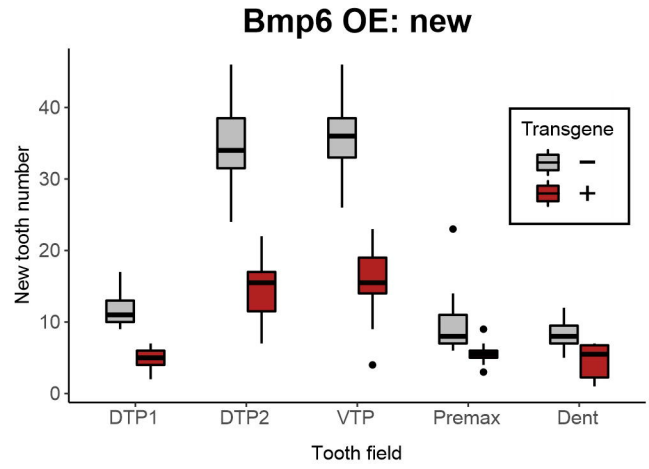
Bmp6 OE: new
New tooth number
0
10
20
30
40
Transgene
−
+
DTP1
DTP2
VTP
Premax
Dent
Tooth field

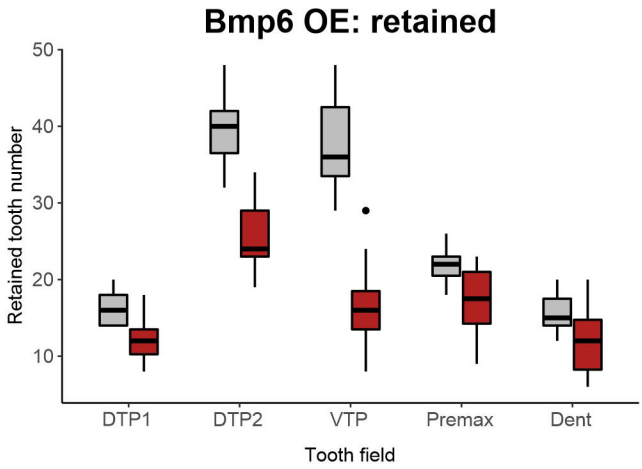
Bmp6 OE: retained
Retained tooth number
10
20
30
40
50
DTP1
DTP2
VTP
Premax
Dent
Tooth field

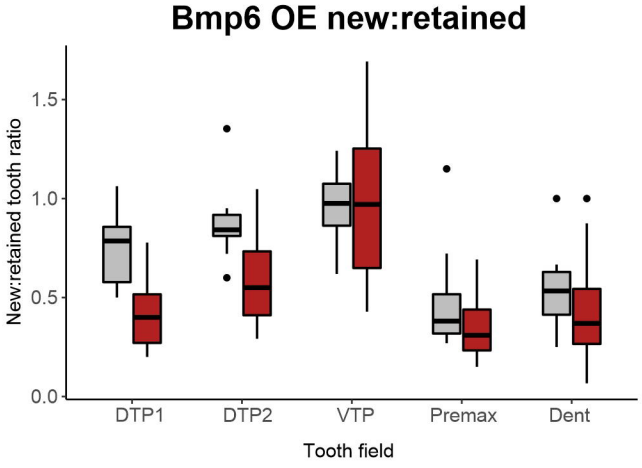
Bmp6 OE new:retained
New:retained tooth ratio
0.0
0.5
1.0
1.5
DTP1
DTP2
VTP
Premax
Dent
Tooth field

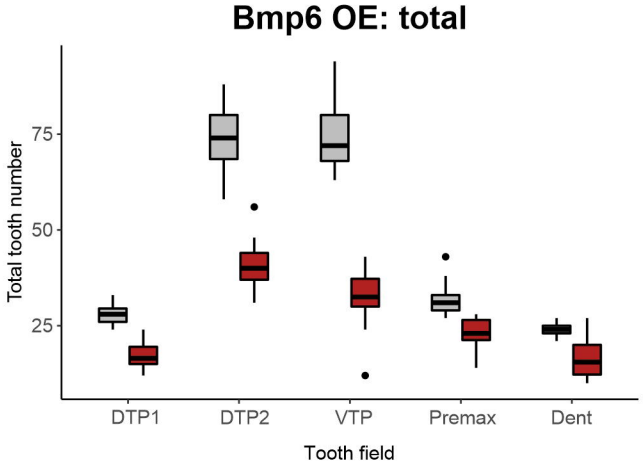
Bmp6 OE: total
Total tooth number
25
50
75
DTP1
DTP2
VTP
Premax
Dent
Tooth field

Stickleback Bmp6 negative control

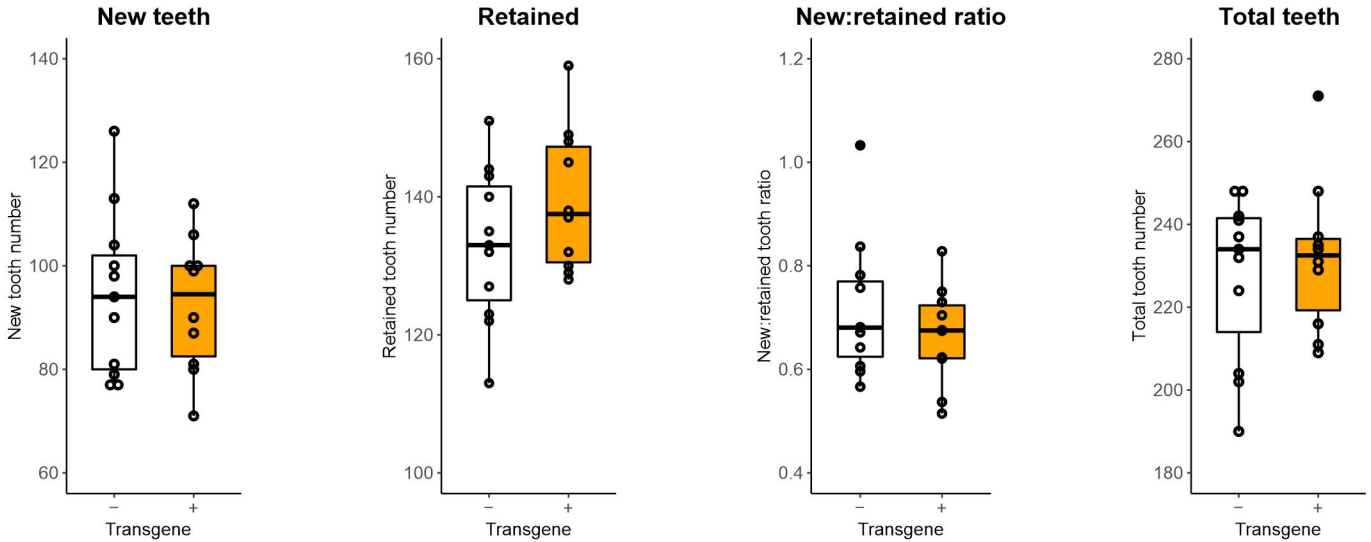

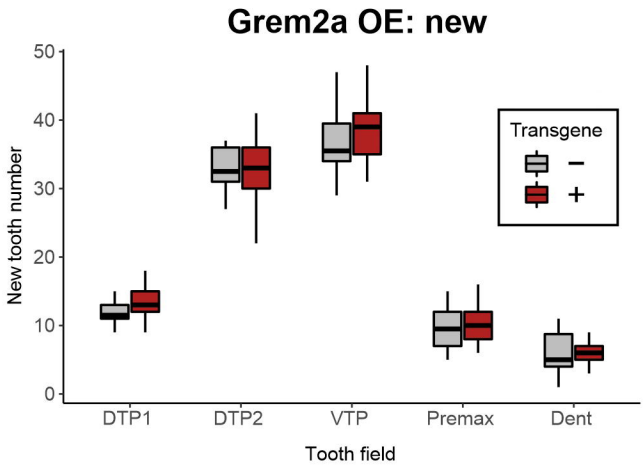
Grem2a OE: new
New tooth number
50
40
30
20
10
0
Transgene
−
+
DTP1
DTP2
VTP
Premax
Dent
Tooth field

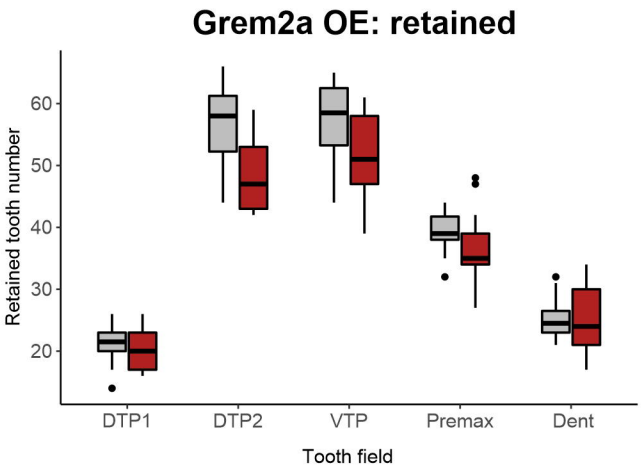
Grem2a OE: retained
Retained tooth number
60
50
40
30
20
DTP1
DTP2
VTP
Premax
Dent
Tooth field

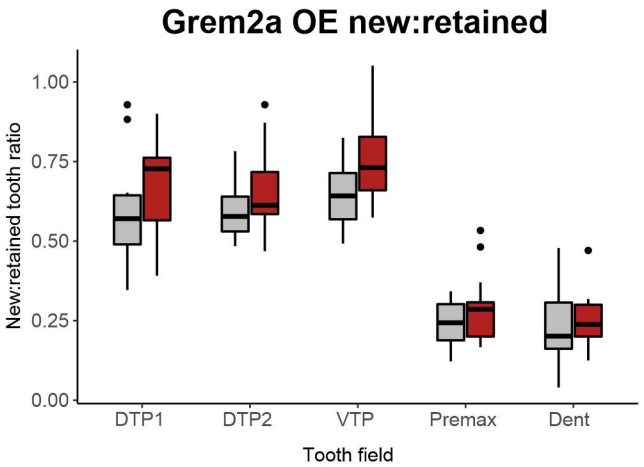
Grem2a OE new:retained
New:retained tooth ratio
1.00
0.75
0.50
0.25
0.00
DTP1
DTP2
VTP
Premax
Dent
Tooth field

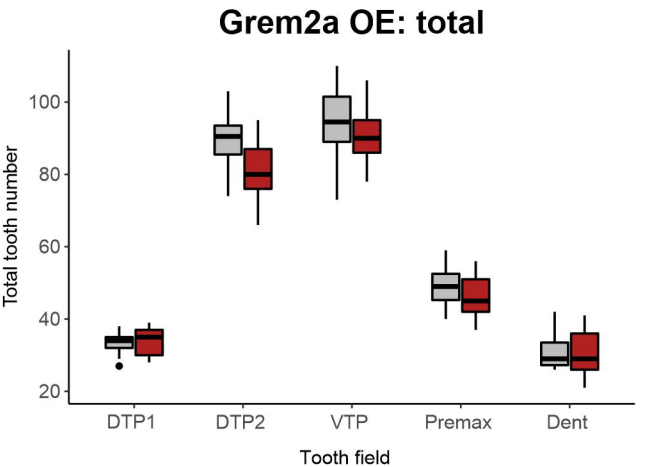
Grem2a OE: total
Total tooth number
100
80
60
40
20
DTP1
DTP2
VTP
Premax
Dent
Tooth field